Supplementary Material

Cascade Biocatalysis for Enantioselective Reconstruction of Both Enantiomers of Phenylalaninol from Biobased L-Phenylalanine

Xue Han,[a, b] Yunyi Li,[a] Tian Xie,[a] Lili Gao,[c] Shuangping Huang,*[a] Hang Gao,*[a] Jiandong Zhang,*[a]

[a] *Department of Biological and Pharmaceutical Engineering, College of Chemistry and Chemical Engineering, Taiyuan University of Technology, Taiyuan 030024, Shanxi, China*

[b]*College of Artificial Intelligence, Taiyuan University of Technology, Taiyuan, Shanxi 030024, China*

[c]*College of Environment and Ecology, Taiyuan University of Technology, Taiyuan, Shanxi, 030024, China*

**Corresponding author:*

Phone: +86-0351-6018534; Fax: +86-0351-6018534

E-mail: zhangjiandong@tyut.edu.cn; huangshuangping@tyut.edu.cn;

hanggao@tyut.edu.cn

Table of contents

1. Bacterial strains, molecular biology reagents and chemicals

E. coli T7 super-competent cells was obtained from New England Biolabs (Beijing, China). The plasmids pET28a, pETduet-1, pCDFduet-1 and pRSFduet-1 for the heterogeneous expression studies were obtained from Novagen (Shanghai, China). Molecular biological reagents, such as T4 DNA ligase and restriction endonuclease were from New England Biolabs (Beijing, China). Plasmid isolation kit was from Tiangen (Shanghai, China). L-phenylalanine **1**a, phenylacetaldehyde **3**a, 4-chlorobenzeneacetaldehyde **3**b, 3-chlorobenzeneacetaldehyde **3**c, 2-chlorobenzeneacetaldehyde **3**d, 4-bromobenzeneacetaldehyde **3**e, benzenepropanal **3**f, 3-(4-bromophenyl)propanal **3**g, 3-(3-chlorophenyl)propionaldehyde **3**h, benzaldehyde **3**i, 4-chlorobenzaldehyde **3**j, 3-bromobenzaldehyde **3**k, 4-methoxybenzaldehyde **3**l, L-phenylglycinol (*S*)-**5**a, D-phenylglycinol (*R*)-**5**a, 2-phenylethylamine **6**, 2-phenylethanol **7**, Pyridoxal-5'-phosphate (PLP), L/D-Alanine and *S*/*R*-phenethylamine were from Energy Chemical (Shanghai, China). Tryptone, yeast extract, isopropyl β-D-thiogalactoside (IPTG), kanamycin, ampicillin, streptomycin and Taq plus DNA polymerase were from Sangon Biotech (Shanghai, China). All other chemicals were of analytical grade and were commercially available.

2. Construction of recombinant *E. coli* cells

All the primers (Table S1) used in this study were synthesized by Tsingke (Beijing, China). All the constructed recombinant *E. coli* strains were listed in Table S2.

For *E. coli* (pET28a-LAAD), the gene of L-amino acid deaminase (LAAD) from *Proteus mirabilis*[1] was synthesized by Tsingke (Beijing, China), and the codon of the LAAD gene sequence was optimized. PCR program settings: initial denaturation at 95°C for 5 min followed by 30 cycles of denaturation at 95°C for 40 s, annealing at 68°C for 40 s, extension at 72°C for 1 min and followed by a final extension at 72°C for 10 min. The PCR product of LAAD genes were isolated and digested with corresponding restriction endonucleases (*Nde* I, *Xho* I), ligated into the pET28a vector to form the recombinant plasmid pET28a-LAAD. The recombinant plasmid pET28a-LAAD was transformed into the competent *E. coli* T7 to form *E. coli* (pET28a-LAAD).

For *E. coli* (pET28a-ARO10), the gene of α-keto acid decarboxylase (ARO10) from *Saccharomyces cerevisiae*[2] was synthesized by Tsingke (Beijing, China), and the codon of the ARO10 gene sequence was optimized. PCR program settings: initial denaturation at 95°C for 5 min followed by 30 cycles of denaturation at 95°C for 40 s, annealing at 68°C for 40 s, extension at 72°C for 1 min and followed by a

final extension at 72°C for 10 min. The PCR product of ARO10 genes were isolated and double-digested with corresponding restriction endonucleases (*BamH* I, *Hind* III), and ligated into the pET28a at the *BamH* I /*Hind* III sites to form the recombinant plasmids pET28a-ARO10. In addition, the recombinant plasmid pET28a-ARO10 was transformed into the competent *E. coli* T7 to form *E. coli* (pET28a-ARO10).

For *E. coli* (pET28a-BALs), the genes of benzaldehyde lyases (BALs) (Table S3) from GenBank was synthesized by Tsingke (Beijing, China), and the codon of the BALs genes sequences were optimized. PCR program settings: initial denaturation at 95°C for 5 min followed by 30 cycles of denaturation at 95°C for 40 s, annealing at 68°C for 40 s, extension at 72°C for 1.5 min and followed by a final extension at 72°C for 10 min. The PCR product of BALs genes were isolated and digested with corresponding restriction endonucleases (*Nde* I-*Xho* I), ligated into the pET28a vector to form the recombinant plasmid pET28a- BALs. The recombinant plasmid pET28a- BALs was transformed into the competent *E. coli* T7 to form *E. coli* (pET28a-BALs).

For *E. coli* (pETDuet-LAAD), the plasmid pET28a-LAAD was used as template for gene amplification of LAAD by PCR. The PCR product of LAAD genes were isolated and digested with corresponding restriction endonucleases (*Nde* I, *Xho* I), ligated into the pETDuet-1 vector to form the recombinant plasmid pETDuet-LAAD. The recombinant plasmid pETDuet-LAAD was transformed into the competent *E. coli* T7 to form *E. coli* (pETDuet-LAAD). The recombinant *E. coli* (pRSFduet-LAAD) and *E. coli* (pCDFduet-LAAD) was also constructed as described above.

For *E. coli* (pETDuet-ARO10), the plasmid pET28a-ARO10 was used as template for gene amplification of ARO10 by PCR. The PCR product of ARO10 genes were isolated and digested with corresponding restriction endonucleases (*BamH* I, *Hind* III), ligated into the pETDuet-1 vector to form the recombinant plasmid pETDuet-ARO10. The recombinant plasmid pETDuet-ARO10 was transformed into the competent *E. coli* T7 to form *E. coli* (pETDuet-ARO10). The recombinant *E. coli* (pRSFduet-ARO10) and *E. coli* (pCDFduet-ARO10) was also constructed as described above.

For *E. coli* (pETDuet-RpBAL), the plasmid pET28a-RpBAL was used as template for gene amplification of RpBAL by PCR. The PCR product of RpBAL genes were isolated and digested with corresponding restriction endonucleases (*BgI* II, *Xho* I), ligated into the pETDuet-1 vector to form the recombinant plasmid pETDuet-RpBAL. The recombinant plasmid pETDuet-RpBAL was transformed into the competent *E. coli* T7 to form *E. coli* (pETDuet-RpBAL).

For *E. coli* (pRSFduet-RpBAL), the plasmid pET28a-RpBAL was used as template for gene amplification of RpBAL by PCR. The PCR product of RpBAL genes were isolated and digested with corresponding restriction endonucleases (*BamH* I, *Hind* III), ligated into the pRSFduet-1 vector to form the recombinant plasmid pRSFduet-RpBAL. The recombinant plasmid pRSFduet-RpBAL was transformed into the competent *E. coli* T7 to form *E. coli* (pRSFduet -RpBAL).

For *E. coli* (pETDuet-ARO10-LAAD), the plasmid pET28a-ARO10 was used as template for gene amplification of ARO10 by PCR. The PCR product of ARO10 genes were isolated and double-digested with corresponding restriction endonucleases (*BamH* I, *Hind* III), and ligated into the pETDuet-LAAD at the *BamH* I/*Hind* III sites to form the recombinant plasmids pETDuet-ARO10-LAAD (known as EAL). In addition, the recombinant plasmid pETDuet-ARO10-LAAD was transformed into the competent *E. coli* T7 to form *E. coli* (pETDuet-ARO10-LAAD) which was named *E. coli* (EAL).

For *E. coli* (pCDFDuet-RpBAL-LAAD), the plasmid pET28a-RpBAL was used as template for gene amplification of RpBAL by PCR. The PCR product of RpBAL genes were isolated and double-digested with corresponding restriction endonucleases (*BamH* I, *Hind* III), and ligated into the pCDFDuet-LAAD at the *BamH* I /*Hind* III sites to form the recombinant plasmids pCDFDuet-RpBAL-LAAD (known as CRL). In addition, the recombinant plasmid pCDFDuet-RpBAL-LAAD was transformed into the competent *E. coli* T7 to form *E. coli* (pCDFDuet-RpBAL-LAAD) which was named *E. coli* (CRL). The recombinant *E. coli* (pRSFduet-RpBAL-LAAD) was also constructed as described above.

For *E. coli* (pETDuet-ARO10-RpBAL), the plasmid pET28a-ARO10 was used as template for gene amplification of ARO10 by PCR. The PCR product of ARO10 genes were isolated and double-digested with corresponding restriction endonucleases (*BamH* I, *Hind* III), and ligated into the pETDuet- RpBAL at the *BamH* I /*Hind* III sites to form the recombinant plasmids pETDuet-ARO10-RpBAL (known as EAR). In addition, the recombinant plasmid pETDuet-ARO10-RpBAL was transformed into the competent *E. coli* T7 to form *E. coli* (pETDuet-ARO10-RpBAL) which was named *E. coli* (EAR).

For *E. coli* (EAL-RR), the constructed recombinant plasmids pETDuet-ARO10-LAAD and pRSFduet-RpBAL were simultaneously transformed into the competent *E. coli* T7 to form the recombinant *E. coli* (pETDuet-ARO10-LAAD/ pRSFduet-RpBAL), designated as *E. coli* (EAL-RR). The recombinant *E. coli* (EAR-CL), *E. coli* (RRL-EA), *E. coli* (RRL-CA), *E. coli* (CRL-EA) and *E. coli* (CRL-RA) was also constructed as described above.

For *E. coli* (EA-CL-RR), the constructed recombinant plasmids pETDuet-ARO10, pCDFduet-LAAD and pRSFduet-RpBAL were simultaneously transformed into the competent E. coli T7 to form the recombinant *E. coli* (pETDuet-ARO10/ pCDFduet-LAAD/pRSFduet-RpBAL), designated as *E. coli* (EA-CL-RR). The recombinant *E. coli* (EL-CA-RR) were also constructed as described above.

3. Supplementary Sequence information

Protein sequence of LAAD:
MNISRRKLLLGVGAAGVLAGGAALVPMVRRDGKFVEAKSRASFVEGTQGALPKEADVVIIGA
GIQGIMTAINLAERGMSVTILEKGQIAGEQSGRAYSQIISYQTSPEIFPLHHYGKILWRGMNEKIG
ADTSYRTQGRVEALADEKALDKAQAWIKTAKEAAGFDTPLNTRIIKGEELSNRLVGAQTPWTV
AAFEEDSGSVDPETGTPALARYAKQIGVKIYTNCAVRGIETAGGKISDVVSEKGAIKTSQVVLA
GGIWSRLFMGNMGIDIPTLNVYLSQQRVSGVPGAPRGNVHLPNGIHFREQADGTYAVAPRIFTS
SIVKDSFLLGPKFMHLLGGGELPLEFSIGEDLFNSFKMPTSWNLDEKTPFEQFRVATATQNTQHL
DAVFQRMKTEFPVFEKSEVVERWGAVVSPTFDELPIISEVKEYPGLVINTATVWGMTEGPAAGE
VTADIVMGKKPIIDPTPFSLDRFKK

Protein sequence of ARO10:
MAPVTIEKFVNQEERHLVSNRSATIPFGEYIFKRLLSIDTKSVFGVPGDFNLSLLEYLYSPSVESA
GLRWVGTCNELNAAYAADGYSRYSNKIGCLITTYGVGELSALNGIAGSFAENVKVLHIVGVAK
SIDSRSSNFSDRNLHHLVPQLHDSNFKGPNHKVYHDMVKDRVACSVAYLEDIETACDQVDNVI
RDIYKYSKPGYIFVPADFADMSVTCDNLVNVPRISQQDCIVYPSENQLSDIINKITSWIYSSKTPA
ILGDVLTDRYGVSNFLNKLICKTGIWNFSTVMGKSVIDESNPTYMGQYNGKEGLKQVYEHFEL
CDLVLHFGVDINEINNGHYTFTYKPNAKIIQFHPNYIRLVDTRQGNEQMFKGINFAPILKELYKR
IDVSKLSLQYDSNVTQYTNETMRLEDPTNGQSSIITQVHLQKTMPKFLNPGDVVVCETGSFQFS
VRDFAFPSQLKYISQGFFLSIGMALPAALGVGIAMQDHSNAHINGGNVKEDYKPRLILFEGDGA
AQMTIQELSTILKCNIPLEVIIWNNNGYTIERAIMGPTRSYNDVMSWKWTKLFEAFGDFDGKY
TNSTLIQCPSKLALKLEELKNSNKRSGIELLEVKLGELDFPEQLKCMVEAAALKRNKK

Protein sequence of BMTA:
MSLTVQKINWEQVKEWDRKYLMRTFSTQNEYQPVPIESTEGDYLIMPDGTRLLDFFNQLYCVN
LGQKNQKVNAAIKEALDRYGFVWDTYATDYKAKAAKIIIEDILGDEDWPGKVRFVSTGSEAVE
TALNIARLYTNRPLVVTREHDYHGWTGGAATVTRLRSYRSGLVGENSESFSAQIPGSSYNSAVL
MAPSPNMFQDSDGNLLKDENGELLSVKYTRRMIENYGPEQVAAVITEVSQGAGSAMPPYEYIP
QIRKMTKELGVLWINDEVLTGFGRTGKWFGYQHYGVQPDIITMGKGLSSSSLPAGAVLVSKEIA
AFMDKHRWESVSTYAGHPVAMAAVCANLEVMMEENFVEQAKDSGEYIRSKLELLQEKHKSIG
NFDGYGLLWIVDIVNAKTKTPYVKLDRNFTHGMNPNQIPTQIIMKKALEKGVLIGGVMPNTM
RIGASLNVSRGDIDKAMDALDYALDYLESGEWQ

Protein sequence of CV2025:
MQKQRTTSQWRELDAAHHLHPFTDTASLNQAGARVMTRGEGVYLWDSEGNKIIDGMAGLWC
VNVGYGRKDFAEAARRQMEELPFYNTFFKTTHPAVVELSSLLAEVTPAGFDRVFYTNSGSESV

DTMIRMVRRYWDVQGKPEKKTLIGRWNGYHGSTIGGASLGGMKYMHEQGDLPIPGMAHIEQ
PWWYKHGKDMTPDEFGVVAARWLEEKILEIGADKVAAFVGEPIQGAGGVIVPPATYWPEIERI
CRKYDVLLVADEVICGFGRTGEWFGHQHFGFQPDLFTAAKGLSSGYLPIGAVFVGKRVAEGLIA
GGDFNHGFTYSGHPVCAAVAHANVAALRDEGIVQRVKDDIGPYMQKRWRETFSRFEHVDDVR
GVGMVQAFTLVKNKAKRELFPDFGEIGTLCRDIFFRNNLIMRACGDHIVSAPPLVMTRAEVDE
MLAVAERCLEEFEQTLKARGLA

Protein sequence of RbTA:
MNQLTILEAGLDEIICETVPGEAIQYSRYSLDRTSPLAGGCAWIEGAFVPAAAARISIFDAGFGHS
DVTYTVAHVWHGNFFRLEDHVERFLAGAEKMRIPMPATKAEIMDLMRGCVSKSGLREAYVN
VCVTRGYGRKPGEKTLEALESQLYVYAIPYLWVFSPIRQIEGIDAVIAQSVRRSPANVMDPWIK
NYQWGDLVRATFEAQERGARTAFLLDSDGFVTEGPGFNVLMVKDGTVFTAARNVLPGITRRT
ALEIARDFGLQTVIGDVTPEMLRGADEIFAATTAGGVTPVVALDGAPVGAGVPGDWTRKIRTR
YWQMMDEPSDLIEPVSYI

Protein sequence of ArTA:
MTSEIVYTHDTGLDYITYSDYELDPANPLAGGAAWIEGAFVPPSEARISIFDQGYLHSDVTYTV
FHVWNGNAFRLDDHIERLFSNAESMRIIPPLTQDEVKEIALELVAKTELREAFVSVSITRGYSSTP
GERDITKHRPQVYMYAVPYQWIVPFDRIRDGVHAMVAQSVRRTPRSSIDPQVKNFQWGDLIRA
VQETHDRGFEAPLLLDGDGLLAEGSGFNVVVIKDGVVRSPGRAALPGITRKTVLEIAESLGHE
AILADITLAELLDADEVLGCTTAGGVWPFVSVDGNPISDGVPGPITQSIIRRYWELNVESSSLLTP
VQY

Protein sequence of CepTA:
MASMDKVFAGYQSRLRVLEASTNPLAQGVAWIEGELVPLSQARIPLMDQGFLHSDLTYDVPAV
WDGRFFRLDDHISRLEKSCSKLRLKLPLPRDEVKRVLVDMVARSGIRDAFVELIVTRGLTGVRG
AGRPEDLVNNLYMFLQPYLWVMPPETQLVGGSAVITRTVRRTPPGSMDPTVKNLQWGDLTRA
LLEASDRGASYPFLTDGDANITEGSGYNIVLIKDGAIHTPDRGVLEGVTRKTVFDIAKANGFEV
RLEVVPVELAYRADEIFMCTTAGGIMPITSLDGQPVNGGQIGPITKKIWDDYWALHYDPAFSFEI
KYDEAGASTNGVNGVHK

Protein sequence of MVTA:
MGIDTGTSKVALVEPGAIREDTPAGSVIQYSDYEIDYSSPFAGGVAWIEGEYLPAEDAKISIFDTG
FGHSDLTYTVAHVWHGNIFRLGDHLDRLLDGARKLRLDSGYTKDELADITKKCVSLSQLRESF
VNLTITRGYGKRKGEKDLSKLTHQVYIYAIPYLWAFPPAEQIFGTTAVVPRHVRRAGRNTVDPTI
KNYQWGDLTAASFEAKDRGARTAILMDADNCVAEGPGFNVCIVKDGKLASPSRNALPGITRKT
VFEIAGAMGIEAALRDVTSHELYDADEIMAVTTAGGVTPINTLDGVPIGDGEPGPVTVAIRDRF
WALMDEPGPLIEAIQY

Protein sequence of PaBAL:
MSSPEARYTGGDLLAQTLHDAGVTKIFALHGGHHEALFKGCIDQGIDLIDFRHEAAAGHAADA
YARTTGKLGVCIITAGPGFTNAISAIANAQLDASPVLFLIGAPPLREVETNPLQGGIDQIAMARPA
AKWALSIPSTERVRDLTAMAIRKAMTGRKGPVVLEIPIDILHMSVTGAQATPSAGLAVRPQPAPA
PEEVAALAELLLRAERPVIVAGLESASAATAVALRALVAKLPLPVFAKPQAYGLLPAGHACDAG

AAGNLAVLPIIGAGAPDLVILLGARLGLMLGGRSGALVPHDAHVVQIYSDASEIGRLRDIDLPIA
ADCAQTLTALTKALAAVDLPDTSAWTARAAGAKALAASAWPDAEVAGGIHPYHAAKAVANA
AGQDAAYVFDGGESSSWGTATVAVDAPARVLSHGYLGCLGIGPGFAIGMQIAHPDRRVVQVTG
DGAMGFHIQEFDTMVRHRLPIVTVILNNQVWGMSIHGQQMMYGANYNVITKLGSTQYASIAA
AFGCHAERVTAFAEIAPAMARAFASGKPALVEIMTDADVVHPATVAMLGQLAEGSRDIMIPYYE
NIAAS

Protein sequence of RpBAL:
MAEQDRLVGGQLLAKTLKAAGVSQAFALHGGHLEALLKGCIEEDIALIDFRHESSAGHAADA
YARATGKLGVCIVTAGPGFTNALSAMTNAQLDGSPVLFIVGAPPLREIETNPLQGGIDQVAIARP
AVKWAFSIPSTERIADLTAMAIRKAMTLPRGAVLLEVPIDVLHMSVSASRATPPAGVGVNPRPAP
APAEVTRLVELLRAAKRPVLIAGNGAANHETAEALRALCARVPLPVFTKSLAAGILPPGHLCNG
GAAGNLALLPMLGIDRPDLVILLGGKLGLLLGGRSGALVPHGATLVQIHGDAAEMGRIRDVDL
PILADCTEATRALDAALKDDQFNELEGWRAKAVSATGLFATMFPDRETTQGIHPYHAARAVAE
TAGPGAMYVFDGGESASWGAAAAVVDRPGAVISHGYLGCLGIGPGFAIGAQIAAPDRRVIHLT
GDGAFGFHLQELDTMVRHRLPIITVILNNEVWGMSIHGQQIMFGSNYHVISKLGGTHFANIAQ
AFGCHAERVTRFADLAPALERAFASSGPAFIEVMTDADVVHPVTVAMLGQVQEGSNDVLIPYY
ENIPADTA

Protein sequence of AbBAL:
MNEVVSRMLTGGDLIAGVLAKAGVKHAFALHGGHLEALLKGCIDNQIALHDFRHESSAGHAA
DAYARATGELGVCIITAGPGFTNAISAIVNAHLDASPVLFLIGAPPLRELETNPLQGGFDQVAMA
LPAVKWTHRATNTERLAELTAMAIRKATTGRRGPVLMELPIDVLHIAVPQSAATAPTGLAVHPR
PAPSPAETEALLALLAGARRPAIIAGGEATQCGAGDALRRFAERSGIPVFANTRGLGLLPSDHPL
SGHGAGNLGALVATGGEAPDVVLLLGARLGLFLGGRSGGIVPNTAKVAQIYSDASEIGRLRDID
VPIAADCAIALEALLAASAKTRWSVDAAWVKRATAMQGFAQQMYPATDAENGVHPYHAAAA
VMRAAGPEAGYVFDGGEAASWAGDCVRVSGPGRVLSHGYLGCLGIGPGFAIGLQTAFPQRRVI
HLTGDGAAGFHLPEFDTMVRHRLPIVTVILNNRVWGMSIHGQQIMYGANYSAITRLGETRYSS
VAAGFGCHAEYVTRFEDIAPAMERALKSGKPACVEILTDEAVIHPITLAMLGKTAEGSNDVVVP
YYENIKA

Protein sequence of CnBAL:
MDRKNGGLLLAEALRHAGVEKIFALHGGHLEALFRGCLEQDIELVDFRHESSAGHAADAYAR
VTGKLGVCVVTAGPGFTNAVSAIANAQLDGIPVLFIVGAPPLREAETNALQGGLDQIAMSATAT
KWAHRITNTERIPDLTAMAIRKAMTGRKGAVLLELPIDVLHMSVDASRATTPTGTATPPRPHGS
PDEVRRVLDLLHAAKRPAIVCGVEAAHARCGEALAHLAETTGVPVFATARGMGVLPAAHRLN
GQAAANLALLGDDVPDVILLLGQRLGLRMGGRGNSLLPRSATLMQVHQDAAEIGRIRDIAVAI
SADSGAVCEQLAEAAAQRSWPQREAWCARAVAAQHILDERYPERETRGGIHPYHAAKAAVAA
AGDAIFVLDGGEAASWAAHHVRANQPGEVIGHGYLGCLGTGPGHAIGAQTAAPGKRVMQITG
DGAMGFHIGEFDIMVRRALPIVTVVLNNQVWGMSIHGQQIMYGPDYSAISKLGDTQYARIAEA
FGCHGERVTRHEDIAAAIERAFCSGKPACVEIMIDPDVVHPVTTSALGMVEAGSGDTLIPYYEN
IPAA

Protein sequence of RhBAL:

MSLGGRTVPNSDTSVDGGELVAKTLHSAGVTRIFALHGGHLESFYRGCAQHQLELVDFRHEAS
AGHAAEAYARVTGQIGVCAITAGPGFANALPAILNAFVDASPTLFLIGAPPLREKETNELQGGFD
QLAIARSSAKWAVSITNVERTPDLLAAAIRRATTGRRGPVVVELPIDVLHMITPADRVTQPSGLS
VHPRPAPSRQELADLRTKLLAAKRPAIVVGGDARFSDCEAILAKFAERAGIPVFASKRGLGILPD
THPCDAHDAANLGLLASSGSPRPDLVILAGTRMGLFLGGSGFGVLPEDAQLVQIYSDPGEIGRI
RDVDLAISADVSAVLECLDDATAEDQWPDWTTWRDLAVDQKNKRAEVFPDPESAGGIHPFHA
MAEVAAVAGSEAVYAIDGGEAGQWAVQHARTDGPGRVITTGYFGGLGVGPGFAIGAQVAAPD
RRVVLVAGDGSFGFHLQELDIMVHNGFPIVTIVLNNEIWGMSLHGQEIMYGKGYNVISKLGGR
NYAEIARAFGCHAERVTNFTELRPALQRAFDSGTAACVEIMTDPEVVSPGLIAMLGDVDSDTPH
IVVPYYENIPL

Protein sequence of BrBAL:
MSTRNSVALRVTGGELLARTLKQAGVTDIFALHGGHLEGFLFHCAQMTLNLIDCRHEASAGHA
ADAYARVSRELGVCVVTAGPGFTNVLSAIVNAQLDSIPTLFIVGAPPLRESETNPLQGGFDQVA
MAAPGAKWSVRITNVERIPDILAMAIRKATTGRMGAVLVEVPIDVMHMDVAAEDVSAPIGLTV
HPRPAPSKPELDAALDILRAAKRPVIIAGIEATRGMTDRAFTDFAEKLGVPVFVSKRAVGILPSG
HPLEGHDQSNLAALTGDDRPDAVLMLGARMGLYLGGRRNGILPKEAKLIQVHSDAMELARLH
EVALPIVADVGATIEALTERASGIAWPDRSAWASKVTALKQRHAALYPSKDSSNGVHPFHAAAE
IARVAGPQAIYALDGGEAGHWAAIHARTDRAGHLLATGYLGCLGVSPGFAIGAQIAAPSRRVVL
IAGDGGIGFHIQELDTMVRHKLPIVSIVFNNGIWGMSRNGQQMMYGANYTSITTLSGTRYAAIA
EAFGCASEVVRRFDDIAPALQRALAANVPALIEIIVDPAVVNPVTVAAVGKPENDPEQILIPYYE
NIRRP

Protein sequence of AgBAL:
MANQKQVEGGELVARTLRAAGVEQIFALHGGHLEGFYRACGAHDLKLVDFRHESSAGHAAE
GYARVTGELGVCAITAGPGFANAVPAILNAYVDGSPTLFLIGAPPLREKETNELQGGFDQMAIA
KPMAKWSVSITNVERIPDLLAAAIRHATTGRRGPVVVELPIDVLHMITTEDRVKKPTGLLVRPR
PAAAPRELNEFKDLLLAAKRPAIIVGGDARFSNCEAALLEFADNSGIPVFSSKRGLGLLPSGHRS
EGHEASNLAGLSANGSAGPDLVVLAGTRLGLFLGGSGFGVIPEDAKIVQIYSDAGEIGRIRDVD
LAIAADVRTVFEGLNGTIAKDEYPVWDEWRSLAVSLQHHHAASYPETENERGIHPFHAAAALS
EVAGPEAVYAIDGGEAGQWAAQQARTSGPGRVITTGYFGGLGVSPGYAIGAQIAAPERRVAVVT
GDGSFGFHLQELDIMVNRNLPIVTLILNNEVWGMSIHGQQIMYGKDYSAISELPGRNYAAIARA
FGCHAERVTSFDDLKPALERAFEAGIPAVVEVMTDPEVVSPGLINMLGTVEDESQQIMVPYYEN
IPR

Protein sequence of RbBAL:
MTRQENRPDGGELLARTLKAAGVEEIFALHGGHLESFWQGCVRHGLRLTDFRHESSAGHAAD
GYARTSGRLGVCAVTSGPGFTNVISAITNAYLDGVPVLFIVGSPPLRDVETNPLQGGIDQVAMA
APTTKWAHRITHAERIPELTAQAIRTCLNGRPGPVLLDLPIDVLHTPVAEARVRAATGLNARTAP
APAPAEVAAIIDLLKTARRPAIFVGNGIRFARAEGELRRFAELAGIPVFCGGHGYGALPYDHPLW
CKDLALLGLLGMTGQPGIDALLAVGARFGLFSGGRGEAIVPSGIAIAQVDLHAPELGRLREVK
VPVLADARETLRALAEAARDVEWPDWSAWAATAAGLKTMTDGMFGPAPAEQSPIHPHHAMT
MLAGVMPRDALYVLDGGETSAWSHMALKADASWQIIGAGYHGCLGVGPGMAIGAQLAHPG
RRVIQITGDGAIGFHIQEFDTQVRHRLPVVTVIFNNQLWGMSAHGQDLIFGRGRRVIADLAGTR

YADIARAFGCHAERVERLAELAPALERTLAAGRPACVEVMIDPEAVHPSMPAMVGADKPAPNE
IMIPYYDNIVLD

Protein sequence of DeBAL:
MTKNESRPDGGELLVRTLKAAGVEEIFALHGGHLESFWQGCVRHGLRLTDFRHESSAGHAAD
AYARTTGRLGVCVVTSGPGFTNVISAIANAYLDAVPVLFIVSSPPLRDVETNPLQGGIDQVAMA
LPTTKWAHRVTHTERIPELAAQAIRTCMNGRPGPVLLDVPIDVLHIPVDEAKVRPATGLNVRTA
PAPAAEDVAAIIEMLKAAQRPAIFVGNGIRFAKAEGELRRFAEAAGIPVFCGGHGYGALPYDHP
LWGKDLALLGALGMMGQPPLDALLVVGARLGLFTGGRNETIVPNGTPIAHVDLHPAELGRLR
EVKVPVLADARETFRALADAAQTVDWPDWAAWTATATAIKSMTGAMFGPAQPEQSPAHPHH
VMETLSAAMPRDAIYVLDGGEVSAWSHMALKADASCQIIGAGYHGCLGTGPGMSIGAQIAHP
DKRVVQVTGDGAMGFHIQEFDTQVRHKLPVLTVILNNQLWGMSAHGQDLIYGRSKRVIADLS
GTRYADIAQAFGCHAERVERLADLAPALARALAAGKPACVEVMIDPDVMHPTMPAMVGADN
PGPNEIMIPYYDNIVMD

Protein sequence of MeBAL:
MVDGGELLARSLRAAGVEQVFALHGGHLDSFWTACGRHGIGLIDTRHEAAAGNAADGYART
TGRLGVAVVTSGPGFANGFAALPNAMSDGVPMLMVTSAPPLRELETNEMQGGFDQIAAATPV
TKWAHRIVTTERIPDLVALAVRKAFAGRPGPVLLEIPIDVLFTPVDETAIPQPGSPTVTDRPGPSPA
AVSAAIDRLRSAKRPAIVLGGGTLWSDCGDEIAEFAEKSGIPVFANNRAIGVLPADHPCNGWGV
DSLALLSMTGQPGPDVVVLMGCRMGLLTGGRATSFIPADAAVIQVDLDASEIGRLRPIEVPIVA
DCRETLRALLVAGAADDVQWPDRSAWLAQATAAHGLVEQMYSAAPAVDDGRLHPYHATREA
LRGAGEGAVLVLDGGEAPLWAAMSQHTVAPHRVLNLGYMGFLGIGQGFAIGAQIAEPDRRVM
QVTGDGSYGFHIQELDTMVRHRLPIVTVVINNACWGMSIHGQDAIYGEGNDVITRLADTDYH
EVARAFGGYGERVTQLDEIAPAVEKAFASGLPACINVAVAPGVVHPMTTAMLGDVDAQNEIVV
PYYENLPKRG

Protein sequence of CsBAL:
MTDSTSLSGGDILAQTLKEAGVDQVFALHGGHLEALLKGCLTRDIALLDFRHESAAGHAADA
YARITGKLGVCAITSGPGFTNGVSAMANAKLDGSPVLFIVGAPPVREVETNALQGGIDQVALA
RPATKWAISVPTTERMADLAAMAIRKAMTHPRGPVLLEVPIDVLHMSVPAERATRPTGVNVQP
RTAPAPESVQALADLLLAAKRPVVIAGNEAANPATAQALQAFTAAHAVPVFTKSLAAGVLPPT
HSHACGPAPGLAALPAIGVERPDLVLLLGGRMGMLLGGRSGAVVPHAAQLVQVHSDAGEIGRI
RDVQLAIAAQADETLKALTAELARRQQTAGHADWLAQARRVNGLFAQQFPEAESASGIHPLH
AARVVAEAAGPDALYVFDGGESASWASAITPVNTPASLLTHGYLGCLGIGPGFAIGGQIACPGR
RVVHLTGDGALGFHIQDFDTMVRHGLPILNVVLNNQVWGMSIHGQQIMYGEDYHAISKLGGT
HYANIAQGFGMHSERVTRFADLEGAVARALAHQGPSFIEVMTAADVVHPVTVSMLGQVPAGS
KDVLIPYYENIVVG

Protein sequence of PfBAL:
MAMITGGELVVRTLIKAGVEHLFGLHGAHIDTIFQACLDHDVPIIDTRHEAAAGHAAEGYARA
GAKLGVALVTAGGGFTNAVTPIANAWLDRTPVLFLTGSGALRDDETNTLQAGIDQVAMAAPIT
KWAHRVMATEHIPRLVMQAIRAALSAPRGPVLLDLPWDILMNQIDEDSVIIPDLVLSAHGARPD
PADLDQALALLRKAERPVIVLGSEASRTARKTALSAFVAATGVPVFADYEGLSMLSGLPDAMR
GGLVQNLYSFAKADAAPDLVLMLGARFGLNTGHGSGQLIPHSAQVIQVDPDACELGRLQGIAL
GIVADVGGTIEALAQATAQDAAWPDRGDWCAKVTDLAQERYASIAAKSSSEHALHPFHASQVI

AKHVDAGVTVVADGALTYLWLSEVMSRVKPGGFLCHGYLGSMGVGFGTALGAQVADLEAGR
RTILVTGDGSVGYSIGEFDTLVRKQLPLIVIIMNNQSWGATLHFQQLAVGPNRVTGTRLENGSY
HGVAAAFGADGYHVDSVESFSAALAQALAHNRPACINVAVALDPIPPEELILIGMDPFA

4. Cultivation of recombinant *E. coli* cells

E. coli T7 cells carrying the desired vectors were inoculated into 4 mL of LB (Luria-Bertani) medium (Tryptone 10 g/L, Yeast extract 5 g/L, NaCl 10 g/L) containing appropriate antibiotics (50 mg/mL kanamycin sulfate, 50 mg/mL streptomycin, 100 mg/mL ampicillin) and incubated for 7 h (37℃, 200 rpm). Then 1.5-2 mL of seed solution was transferred to 50 mL of TB (Terrific Broth) medium (Tryptone 12 g/L, Yeast extract 24 g/L, Glycerol 0.4%, K_2HPO_4 12.54 g/L, KH_2PO_4 2.32 g/L), and when the OD_{600} reached 0.6-0.8, the final concentration of IPTG was added as 0.5 mM. The culture was incubated for 12-14 h at 20℃, 200 rpm, to induce the expression of the desired enzymes. Centrifuge the bacterial solution at 4℃ and 8000 rpm for 10 minutes, and the cells were harvested. Then the cell pellets were resuspended in 100 mM sodium phosphate buffer (pH 7.0-8.0). Enzyme expression was confirmed by SDS-PAGE.

5. Asymmetric reductive amination of α-hydroxy ketone 4a to 5a

To identify suitable ATA biocatalysts, we screened a variety of ATAs available in our laboratory using **4**a as a substrate. The standard reaction mixture was sodium phosphate buffer (100 mM, pH 8.0) containing 5 mM **4**a, 0.1 mM PLP, 100 mM D/L- Ala or 6 mM (*S*/*R*)-PEA, and 20 g cdw/L *E. coli* (ATAs) resting cells. The reaction was incubated for 10 h at 30°C and 200 rpm. The reaction solution (200 μL) was basified with NaOH (10 μL, 10 N) and then fully saturated with NaCl, mixed thoroughly with ethyl acetate (200 μL) containing 2 mM dodecane (internal standard), and then centrifuged at 12,000 rpm for 5 min. The resulting organic phase was dried with anhydrous sodium sulfate and analyzed by GC.

6. Purification and enzyme activity analysis of RpBAL

Overnight cultured *E. coli* (RpBAL) cells were collected by centrifugation at 8000 g for 10 min at 4°C, and the supernatant was discarded. The cell pellet was washed twice with pre-cooled (4°C) Tris-HCl buffer (20 mM, pH 7.5) and resuspended in the same buffer. The cell suspension was placed on ice and sonicated 90 times at 400 W for 4 s with 4 s intervals to yield cell-free extracts. After centrifugation (12,000×*g* and 4°C), the supernatant was stored at -20°C. Protein purification was done *via* metal affinity chromatography. The crude lysate was loaded onto a nickel sepharose column (Sangon Biotech, Shanghai,

China) after equilibration with loading buffer (20 mM Tris-HCl buffer (pH 7.5) and 150 mM NaCl). Non-specifically bound proteins were removed by prewashing with two column volumes of Tris-HCl buffer (pH 7.5) containing 20 mM and 50 mM imidazole. RpBAL was eluted with two column volumes of Tris-HCl buffer (pH 7.5) with 100 mM, 250 mM and 500 mM imidazole and dialyzed against Tris-HCl buffer (pH 7.5) for 24 h at 4°C. Finally, the purified enzyme solutions were stored at 4°C for further use. Purified enzymes were evaluated by SDS-PAGE. The Bradford method[3] was used to determine the protein concentration of the enzyme solution, bovine serum albumin (BSA) was used as standard.

One unit (U) of enzyme activity is defined as the amount of enzyme that catalyzes the conversion of 1 μmol of **4**a from **3**a per minute at 30°C. The reaction mixture (1 mL) consisted of 100 mM sodium phosphate buffer (pH 8.0), 2.5 mM $MgSO_4$, 0.3 mM ThDP, 10% (v/v) DMSO, 30 mM formaldehyde, and a specified amount of purified RpBAL. The reaction was initiated by adding the enzyme, followed by incubation at 30°C for 20 minutes. The production of **4**a from **3**a by RpBAL was quantified using gas chromatography (GC).

7. Effect of pH and temperature on enzyme activity

The effects of pH and temperature on enzyme activity were analyzed using 3a as a substrate. To determine the optimal pH of purified RpBAL, two buffer systems were employed: a sodium phosphate buffer (100 mM) with a pH range of 6.0 to 8.0, and a glycine-NaOH buffer (100 mM) with a pH range of 8.0 to 11.0. The optimal temperature for purified RpBAL was assessed by measuring enzyme activity at temperatures from 20°C to 50°C in sodium phosphate buffer (100 mM) at the optimal pH. The enzyme's pH stability was evaluated by incubating it in 1 mL of sodium phosphate buffer (pH 6.0-8.0) and glycine-NaOH buffer (100 mM, pH 9.0-11.0). For thermal stability, the enzyme was kept in 1 mL of sodium phosphate buffer (100 mM, pH 8.0) at temperatures ranging from 4°C to 50°C. Samples were collected at specific time intervals and assayed for residual benzaldehyde lyase activity under standard conditions.

8. Homology model, molecular docking and MD simulations

The homology model of RpBAL were constructed using AlphaFold3,[4] based on its sequence similarity to PfBAL (PDB ID: 2UZ1), with which it shares 38% identity and 56% similarity. Visual inspection and evaluation of the active site were performed using PyMOL (version 2.5) and Caver 3.0.[5] The ionization states of RpBAL/PfBAL and its cofactor THDP were determined using PROPKA3 at pH 7.4.[6] The

substrate, 2-phenylacetaldehyde, was geometry-optimized using the HF/6-31G(d,p) method, and atomic point charges were calculated with the RESP algorithm.[7] Molecular docking of 2-phenylacetaldehyde to RpBAL was conducted using AutoDock Vina with its standard free energy scoring function. The top-ranked docking pose with the lowest binding energy was selected and further analyzed in PyMOL. Following this analysis, the RpBAL-substrate complex was subjected to molecular dynamics (MD) simulations.[8]

MD simulations were performed using Desmond 2021 with the OPLS_2005 force field.[9] The RpBAL-substrate complex was solvated in a cubic box of TIP3P water molecules, extending 15 Å from the protein, under periodic boundary conditions. Sodium and chloride ions were added to achieve a physiological concentration of 0.15 M NaCl, with additional ions included to neutralize the system's net charge. The system was equilibrated using a multi-step protocol. Initially, it was relaxed with a 200 ps Brownian dynamics simulation. This was followed by minimization and heating stages with restraints on solute heavy atoms. The production simulation was then run for 200 ns in the NPT ensemble at 300 K and 1 atm, employing the Nose-Hoover thermostat and Martyna-Tobias-Klein barostat. Long-range electrostatic interactions were calculated using the particle-mesh Ewald method, with a 12 Å cutoff applied to van der Waals interactions. The SHAKE algorithm was used to constrain bonds involving hydrogen atoms. Trajectory frames were recorded every 50 ps.

Trajectory analysis was conducted to evaluate the stability and flexibility of the RpBAL-substrate complex. The root mean square deviation (RMSD) of the substrate, protein backbone, and root mean square fluctuation (RMSF) of each residue's backbone and side chains were calculated.

9. General procedure for biocatalytic hydroxymethylation of aldehydes 3a-l

A 50 mL reaction vessel was prepared with a 3 mL reaction mixture containing 100 mM sodium phosphate buffer (pH 8.0), 10 mM of aldehyde (**3**a-l), 30 mM HCHO, 2.5 mM $MgSO_4$, 0.3 mM ThDP, 10% (v/v) DMSO, and 20 g CDW L^{-1} of *E. coli* (RpBAL) resting cells. The reactions were conducted at 30°C and 200 rpm for 4 to 24 hours. To assess the conversion of **3**a-l, a 200 μL sample of the reaction mixture was saturated with NaCl and extracted with 200 μL of ethyl acetate containing 2 mM dodecane as the internal standard, followed by centrifugation at 12,000 rpm for 5 minutes. The organic phase was then dried using anhydrous Na_2SO_4 and analyzed by gas chromatography (GC).

10. Preparative scale synthesis of α-hydroxy ketones 3a-l

The standard reaction mixture consisted of 50 mL of sodium phosphate buffer (100 mM, pH 8.0), containing 10 mM of aldehyde (**3**a-l), 30 mM of formaldehyde (HCHO), 2.5 mM of MgSO4, 0.3 mM of ThDP, 10% (v/v) DMSO, and 20 g CDW L^{-1} of *E. coli* (RpBAL) resting cells. The reactions were conducted at 30°C and 200 rpm, and reaction progress was monitored using thin-layer chromatography (TLC). Once the product conversion rate peaked, the reaction mixture was extracted with ethyl acetate (3 × 50 mL). The combined extracts were dried with anhydrous sodium sulfate (Na_2SO_4), concentrated under reduced pressure, and the crude product was purified by silica gel chromatography using a petroleum ether-ethyl acetate (5:1) eluent.

Supplementary ^{1}H-NMR and ^{13}C-NMR data of the products

1-Hydroxy-3-phenylpropan-2-one (4a)

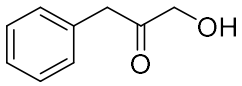

^{1}H NMR (400 MHz, Chloroform-*d*) δ 7.42 – 7.27 (m, 3H), 7.25 – 7.12 (m, 2H), 4.29 (d, *J* = 2.6 Hz, 2H), 3.73 (s, 2H), 3.03 (t, *J* = 4.7 Hz, 1H). ^{13}C NMR (101 MHz, $CDCl_3$) δ 207.33, 132.73, 129.32, 128.97, 127.53, 77.37, 77.05, 76.73, 67.69, 45.84.

1-(4-Chlorophenyl)-3-hydroxy-2-propanone (4b)

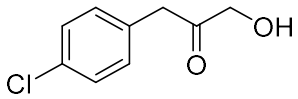

^{1}H NMR (600 MHz, Chloroform-*d*) δ 7.32 (d, *J* = 8.4 Hz, 2H), 7.15 (d, *J* = 8.4 Hz, 2H), 4.30 (s, 2H), 3.70 (s, 2H), 3.04 (s, 1H). ^{13}C NMR (101 MHz, Chloroform-*d*) δ 206.77, 133.55, 131.10, 130.70, 129.08, 67.80, 44.85.

1-(3-Chlorophenyl)-3-hydroxy-2-propanone (4c)

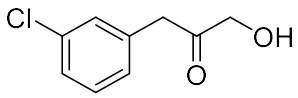

^{1}H NMR (400 MHz, Chloroform-*d*) δ 7.34 – 7.28 (m, 3H), 7.14 (s, 1H), 4.34 (s, 2H), 3.74 (s, 2H), 3.02 (s, 1H). ^{13}C NMR (101 MHz, Chloroform-*d*) δ 206.47, 134.74, 134.49, 130.15, 129.50, 127.79, 127.54, 67.85, 45.10.

1-(2-Chlorophenyl)-3-hydroxy-2-propanone (4d)

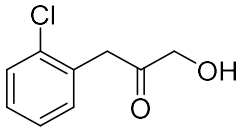

^{1}H NMR (400 MHz, Chloroform-*d*) δ 7.40 (d, *J* = 5.1 Hz, 1H), 7.26 (s, 3H), 4.34 (s, 2H), 3.87 (s, 2H), 3.03 (s, 1H). ^{13}C NMR (101 MHz, Chloroform-*d*) δ 206.31, 134.33, 131.76, 131.28, 129.75, 129.18, 127.27, 68.08, 43.55.

1-(4-Bromophenyl)-3-hydroxy-2-propanone (4e)

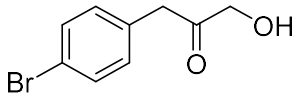

^{1}H NMR (400 MHz, Chloroform-*d*) δ 7.48 (d, *J* = 7.8 Hz, 2H), 7.10 (d, *J* = 7.9 Hz, 2H), 4.30 (d, *J* = 4.5 Hz, 2H), 3.69 (s, 2H), 2.97 (s, 1H). ^{13}C NMR (101 MHz, $CDCl_3$) δ 206.61, 132.06, 131.57, 131.04, 121.64, 77.35, 77.03, 76.72, 67.81, 44.94.

1-Hydroxy-4-phenyl-2-butanone (4f)

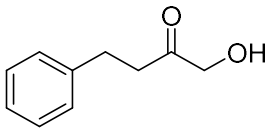

^{1}H NMR (600 MHz, Chloroform-*d*) δ 7.29 (t, *J* = 7.6 Hz, 2H), 7.23 – 7.19 (m, 1H), 7.19 – 7.15 (m, 2H), 4.19 (s, 2H), 3.16 – 3.05 (m, 1H), 2.97 (t, *J* = 7.6 Hz, 2H), 2.73 (t, *J* = 7.6 Hz, 2H). ^{13}C NMR (101 MHz, $CDCl_3$) δ 208.88, 140.17, 128.67, 128.24, 126.47, 77.37, 77.06, 76.74, 68.38, 39.94, 29.59.

4-(4-Bromophenyl)-1-hydroxy-2-butanone (4g)

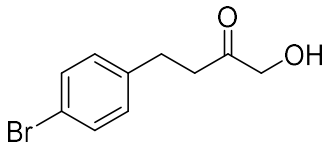

^{1}H NMR (400 MHz, Chloroform-*d*) δ 7.40 (d, *J* = 7.3 Hz, 2H), 7.05 (d, *J* = 7.6 Hz, 2H), 4.19 (d, *J* = 3.9 Hz, 2H), 3.04 (s, 1H), 2.92 (t, *J* = 7.4 Hz, 2H), 2.71 (t, *J* = 7.4 Hz, 2H). ^{13}C NMR (101 MHz, Chloroform-*d*) δ 208.47, 139.15, 131.72, 130.06, 120.27, 68.39, 39.63, 28.86.

4-(3-Chlorophenyl)-1-hydroxy-2-butanone (4h)

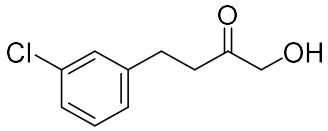

^{1}H NMR (400 MHz, Chloroform-*d*) δ 7.20 (t, *J* = 8.8 Hz, 3H), 7.06 (d, *J* = 6.8 Hz, 1H), 4.21 (s, 2H),

2.95 (t, *J* = 7.4 Hz, 2H), 2.73 (t, *J* = 7.5 Hz, 2H), 1.25 (s, 1H). ^{13}C NMR (101 MHz, $CDCl_3$) δ 208.36, 142.20, 134.40, 129.91, 128.44, 126.70, 126.51, 77.35, 77.04, 76.72, 68.35, 39.54, 29.03.

2-Hydroxyacetophenone (4i)

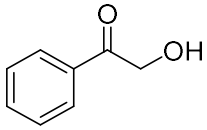

^{1}H NMR (400 MHz, Chloroform-*d*) δ 7.92 (d, *J* = 7.8 Hz, 2H), 7.63 (t, *J* = 7.3 Hz, 1H), 7.50 (t, *J* = 7.6 Hz, 2H), 4.88 (s, 2H), 3.55 (s, 1H). ^{13}C NMR (101 MHz, $CDCl_3$) δ 198.42, 134.32, 133.38, 129.00, 127.72, 77.38, 77.06, 76.74, 65.47.

1-(4-Chlorophenyl)-2-hydroxyethanone (4j)

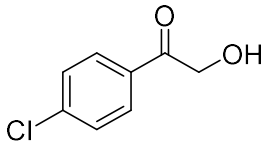

^{1}H NMR (400 MHz, Chloroform-*d*) δ 7.89 (d, *J* = 8.4 Hz, 2H), 7.51 (d, *J* = 8.4 Hz, 2H), 4.87 (s, 2H), 3.48 (t, *J* = 4.5 Hz, 1H). ^{13}C NMR (101 MHz, Chloroform-*d*) δ 197.30, 140.83, 131.71, 129.40, 129.09, 65.44.

1-(3-Bromophenyl)-2-hydroxyethanone (4k)

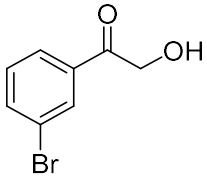

^{1}H NMR (400 MHz, Chloroform-*d*) δ 8.05 (t, *J* = 1.7 Hz, 1H), 7.83 (dt, *J* = 7.7, 1.3 Hz, 1H), 7.76 (dd, *J* = 8.1, 1.9 Hz, 1H), 7.39 (t, *J* = 7.9 Hz, 1H), 4.85 (s, 2H), 3.42 (s, 1H). ^{13}C NMR (101 MHz, Chloroform-*d*) δ 197.31, 137.15, 135.09, 130.78, 130.59, 126.18, 123.35, 65.58.

2-Hydroxy-1-(4-methoxyphenyl)ethanone (4l)

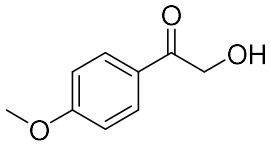

^{1}H NMR (400 MHz, Chloroform-*d*) δ 7.90 (d, *J* = 8.7 Hz, 2H), 6.96 (d, *J* = 8.7 Hz, 2H), 4.82 (d, *J* = 3.8 Hz, 2H), 3.88 (s, 3H), 3.57 (t, *J* = 4.6 Hz, 1H). ^{13}C NMR (101 MHz, Chloroform-*d*) δ 196.72, 164.39, 130.02, 126.37, 114.19, 64.99, 55.58.

11. *In vitro* cascade biocatalysis for conversion of 1a to 5a

The *in vitro* cascade biocataysis was carried out in one-pot with the cell-free extracts of *E. coli* (LAAD),

E. coli (ARO10), *E. coli* (RpBAL), and *E. coli* (BMTA) or *E. coli* (MVTA). For the one-pot concurrent setup, the standard reactions were conducted in 3 mL of 100 mM sodium phosphate buffer at pH 8.0, containing 10 mM of substrate **1**a, 0.3 mM ThDP, 2.5 mM $MgSO_4$, 30 mM formaldehyde (HCHO), 0.1 mM PLP, 200 mM L-alanine (L-Ala), or 12 mM R-phenylethylamine (R-PEA). The reaction mix included 15 mg/mL of each of the enzymes (LAAD, ARO10, and RpBAL) and 20 mg/mL of either BMTA or MVTA, and the mixtures were incubated at 30 °C with shaking at 200 rpm for 15 hours. For the one-pot two-stage approach, the reactions were first conducted under the same conditions without BMTA or MVTA. Once the conversion of product **4**a was maximized, 20 mg/mL of either BMTA or MVTA was added to the reaction mixture. A 200 μL sample of the reaction mixture was basified with 0.1 mL of 10 N NaOH, saturated with NaCl, and extracted with 200 μL of ethyl acetate containing 2 mM dodecane as an internal standard. The mixture was centrifuged at 12,000 rpm for 5 minutes, and the organic phase was dried over anhydrous Na_2SO_4 before analysis by gas chromatography (GC).

12. One-pot two-stage bioconversion of 1a to 5a with the resting cells of *E. coli* (EAL-RR) and *E. coli* (BMTA) or *E. coli* (MVTA)

The standard reactions were carried out in 3 mL sodium phosphate buffer (100 mM, pH 7.0) containing 10 mM **1**a, 10% (v/v) DMSO, 0.3 mM ThDP, 2.5 mM $MgSO_4$, 30 mM HCHO, 200 mM L-Ala or 12 mM *R*-PEA, 0.1 mM PLP, 25 g cdw/L *E. coli* (EAL-RR), and the reactions were incubation at 30°C, and 200 rpm. Once the conversion of **4**a reached maximum, an additional 25 g CDW L^{-1} of *E. coli* (BMTA) or *E. coli* (MVTA) resting cells was introduced into the reaction mixture. The reaction continued at 30°C and 200 rpm for 9 h. A 200 μL sample of the reaction solution was basified with 10 μL of 10 N NaOH and saturated with NaCl, followed by extraction with 200 μL of ethyl acetate containing 2 mM dodecane as an internal standard. The mixture was then centrifuged at 12,000 rpm for 5 minutes. The organic phase was dried with anhydrous Na_2SO_4, and the concentration and enantiomeric excess (*ee*) of compound **5**a were analyzed using GC and HPLC methods.

13. Preparative scale synthesis of 5a

The standard reaction mixture consisted of 100 mL of 100 mM sodium phosphate buffer (pH 7.0), containing 10 mM (165 mg) of **1**a, 10% (v/v) DMSO, 20 mM formaldehyde, 2.5 mM $MgSO_4$, 0.3 mM thiamine diphosphate (ThDP), and either 200 mM L-alanine or 12 mM (*R*)-phenylethylamine (R-PEA).

Additionally, 0.1 mM pyridoxal phosphate (PLP) and 25 g CDW L^{-1} of *E. coli* (EAL-RR) were included. The mixture was incubated at 30 °C and 200 rpm for 6 hours. Once the conversion of **4**a reached its maximum, 25 g CDW L^{-1} of either *E. coli* (BMTA) or *E. coli* (MVTA) resting cells were added, and the reactions continued at the same conditions for an additional 9 hours. Afterward, the cells were removed by centrifugation at 4500×g for 10 minutes at 4 °C. The supernatant was basified to pH > 10 using 10 N NaOH and saturated with NaCl. It was then extracted three times with 50 mL of ethyl acetate. The combined extracts were dried over anhydrous Na_2SO_4, concentrated under reduced pressure, and the crude product was purified by chromatography on silica gel using a petroleum ether-ethyl acetate (3:1) eluent. ^{1}H NMR (400 MHz, Chloroform-*d*) δ 7.30 (t, *J* = 7.3 Hz, 2H), 7.21 (dd, *J* = 17.1, 7.4 Hz, 3H), 3.63 (dd, *J* = 10.7, 3.7 Hz, 1H), 3.45 – 3.34 (m, 1H), 3.12 (dq, *J* = 12.2, 8.4, 6.5 Hz, 1H), 2.79 (dd, *J* = 13.5, 5.1 Hz, 1H), 2.51 (dd, *J* = 13.4, 8.8 Hz, 1H). ^{13}C NMR (101 MHz, Chloroform-*d*) δ 138.73, 129.23, 128.61, 126.44, 66.24, 54.22, 40.84.

14. Chemical synthesis of Solriamfetol

The chemical synthesis of Solriamfetol from compound (*R*)-**5**a was performed using Bhirud's method.[10] In a 10 mL round-bottom flask, combine 1 mL of dichloromethane with 105 mg (0.69 mmol) of (*R*)-**5**a and 59.8 mg (0.95 mmol) of sodium cyanate while stirring the mixture in an ice bath. Gradually add 103 µL (2.35 mmol) of methanesulfonic acid dropwise, ensuring the temperature remains below 5°C. The mixture will thicken once the addition is complete. After removing the ice bath, continue stirring until (*R*)-**5**a is no longer detectable by TLC. Gradually add 20% aqueous sodium hydroxide to adjust the pH of the reaction mixture to 10-11. Transfer the mixture to a separatory funnel, extract the aqueous phase with dichloromethane, and wash the combined organic phases with brine. Next, separate and concentrate the organic phase under reduced pressure. Finally, purify the product by chromatography on silica gel using a dichloromethane-methanol (5:1) eluent. This process yielded Solriamfetol as oil in 91.3% yield (123 mg). ^{1}H NMR (400 MHz, Chloroform-*d*) δ 7.30 (t, *J* = 7.3 Hz, 2H), 7.26 – 7.15 (m, 3H), 4.99 (s, 2H), 4.10 (dd, *J* = 10.7, 3.7 Hz, 1H), 3.90 (dd, *J* = 10.4, 7.4 Hz, 1H), 3.28 (s, 1H), 2.81 (dd, *J* = 13.5, 5.1 Hz, 1H), 2.56 (dd, *J* = 13.4, 8.5 Hz, 1H), 1.40 (s, 2H). ^{13}C NMR (101 MHz, $CDCl_3$) δ 156.97, 138.16, 129.28, 128.62, 126.57, 77.39, 77.07, 76.76, 69.36, 51.78, 40.52.

15. Assay methods

The concentration of **1**a and **2**a was performed with a Shimadzu HPLC LC-10A system equipped with an ultraviolet absorption detector (SPD) and reversed-phase C18 column (4.6 mm×250 mm×5 μm, Phenomenex, Shanghai) at 30°C. The analytical conditions were as follows:

Method A: Column: Luna® 5μm C18 (4.6×250 mm, 5 μm, Phenomenex) Parameter: Detection: UV at 210 nm; The mobile phase consisted of A (0.1% trifluoroacetic acid in acetonitrile) and B (0.1 % trifluoroacetic acid in water) and maintained A: B = 90: 10 for 10 min.; Flow rate: 1 mL/min. The injection volume of each sample was 20 μL.

The concentrations of **4**a-l and **5**a were measured by gas chromatograph. Gas chromatography analysis was carried out with a GC-14C gas chromatography (Shimadzu, Japan) equipped with a flame ionization detector (FID). The analytical conditions were as follows:

Method B: Column: Agilent J&W HP-5 (30 m, 0.32 mm, 0.25 μm). Parameter: injector temperature, 250°C; detector temperature, 275°C; temperature program: column temperature, 120°C, hold 20 min.

Method C: Column: Agilent J&W HP-5 (30 m, 0.32 mm, 0.25 μm). Parameter: injector temperature, 250°C; detector temperature, 275°C; temperature program: column temperature, 140°C, hold 20 min.

Method D: Column: Agilent J&W HP-5 (30 m, 0.32 mm, 0.25 μm). Parameter: injector temperature, 250°C; detector temperature, 275°C; temperature program: column temperature, 150°C, hold 20 min.

Retention times for the α-hydroxy ketones by achiral GC were listed in Table S5. The analytical method for the compound **5**a is **Method B**, with a retention time of 8.342 min.

The enantiomeric excess of **5**a was analyzed using a Shimadzu HPLC system with a CROWNPAK CR (+) column (4×150 mm, 5 μm), where (*R*)-**5**a has a retention time of 14.710 min and (*S*)-**5**a has a retention time of 15.719 min. The analytical conditions were as follows:

Method E: Column: CROWNPAK CR (+) column (4×150 mm, 5 μm). Parameter: Detection: UV at 210 nm; The detection was carried out at 210 nm, and the eluent used was H_2O with perchloric acid at pH 1.30. Flow rate: 0.8 mL/min. The injection volume of each sample was 20 μL.

Table S1. Primers used in this study

Entry	Names	Primers (5'-3')	REA[a]
1	LAAD-F	GGGAATTC***CATATG***AACATTTCACGTCGCAAGCTGCTGC	*NdeI*
2	LAAD-R	CCG***CTCGAG***TTACTTCTTAAAACGATCCAAACTAAACGGGG	*Xho*I
3	ARO10-F	CGC***GGATCC***GATGGCACCTGTTACGATTGAAAAGTTTG	*BamH*I
4	ARO10-R	CCC***AAGCTT***TTACTTCTTATTACGTTTCAGTGCAGCCGC	*Hind*III
5	RpBAL-F	CGC***GGATCC***GATGGCGGAACAAGACCGTC	*BamH*I
6	RpBAL-R	CCC***AAGCTT***TTACGCGGTATCAGCCGGAATGTTCTC	*Hind*III
7	RpBAL-F'	GGA***AGATCT***CATGGCGGAACAAGACCGTCTTG	*BgI* II
8	RpBAL-R'	CCG***CTCGAG***TTACGCGGTATCAGCCGG	*Xho*I

[a] REA: restriction endonuclease

Table S2. Strains and plasmids used in this study

Recombinant *E. coli*	Recombinant plasmids	Enzyme expressed	Ref.
E. coli (LAAD)	pET28a-LAAD	LAAD (*Proteus mirabilis*)	[1]
E. coli (ARO10)	pET28a-ARO10	ARO10 (*Saccharomyces cerevisiae*)	[2]
E. coli (RpBAL)	pET28a-RpBAL	RpBAL (*Rhodopseudomonas palustris*)	this study
E. coli (BMTA)	pET28a-BMTA	BMTA (*Bacillus megaterium* SC6394)	[11]
E. coli (CV2025)	pET28a-CV2025	CV2025 (*Chromobacterium violaceum*)	[12]
E. coli (ArTA)	pET28a-ArTA	ArTA (*Arthobacter*)	[13]
E. coli (RbTA)	pET28a-RbTA	RbTA (*Rhodobacter sp.*140A)	[14]
E. coli (CepTA)	pET28a-CepTA	CepTA (*Capronia epimyces*)	[15]
E. coli (MVTA)	pET28a-MVTA	MVTA (*Mycobacterium vanbaalenii*)	[16]
E. coli (EAL)	pETDuet-ARO10-LAAD	ARO10 and LAAD	this study
E. coli (EAR)	pETDuet-ARO10-RpBAL	ARO10 and RpBAL	this study
E. coli (RRL)	pRSFDuet-RpBAL-LAAD	RpBAL and LAAD	this study
E. coli (CRL)	pCDFDuet-RpBAL-LAAD	RpBAL and LAAD	this study
E. coli (EAL-RR)	pETDuet-ARO10-LAAD pRSFDuet-RpBAL	LAAD, ARO10 and RpBAL	this study
E. coli (EAR-CL)	pETDuet-ARO10-RpBAL pCDFDuet-LAAD	LAAD, ARO10 and RpBAL	this study
E. coli (RRL-EA)	pRSFDuet-RpBAL-LAAD pETDuet-ARO10	LAAD, ARO10 and RpBAL	this study
E. coli (RRL-CA)	pRSFDuet-RpBAL-LAAD pCDFDuet-ARO10	LAAD, ARO10 and RpBAL	this study
E. coli (CRL-EA)	pCDFDuet-RpBAL-LAAD pETDuet-ARO10	LAAD, ARO10 and RpBAL	this study
E. coli (CRL-RA)	pCDFDuet-RpBAL-LAAD pRSFDuet-ARO10	LAAD, ARO10 and RpBAL	this study
E. coli (EA-CL-RR)	pETDuet-ARO10 pCDFDuet-LAAD pRSFDuet-RpBAL	LAAD, ARO10 and RpBAL	this study
E. coli (EL-CA-RR)	pETDuet-LAAD pCDFDuet-ARO10 pRSFDuet-RpBAL	LAAD, ARO10 and RpBAL	this study

Table S3. Benzaldehyde lyase used in this study

Entry	Enzyme	Protein identifier	Organism	Identities
1	PaBAL	WP_135246357.1	*Polymorphobacter arshaanensis*	100.0%
2	**RpBAL**	WP_142882720.1	*Rhodopseudomonas palustris*	68.5%
3	AbBAL	MCC6921341.1	*Alphaproteobacteria bacterium*	65.0%
4	CnBAL	WP_013959462.1	*Cupriavidus necator*	60.1%
5	RhBAL	KXX55911.1	*Rhodococcus sp. LB1*	56.0%
6	BrBAL	MDB5577218.1	*Bradyrhizobium sp.*	53.1%
7	AgBAL	WP_003806000.1	*Arthrobacter globiformis*	53.1%
8	RbBAL	MBK9956574.1	*Rhodocyclaceae bacterium*	52.3%
9	DeBAL	WP_145842972.1	*Denitratisoma sp. DHT3*	53.0%
10	MeBAL	WP_064918042.1	*Mycolicibacterium elephantis*	51.6%
11	CsBAL	WP_087283511.1	*Comamonas serinivorans*	64.0%

Table S4. Retention times for the α-hydroxyketones analysed by achiral GC.

Compound	[min]	Method	Compound	[min]	Method
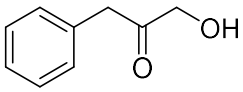 **4**a	6.070	B	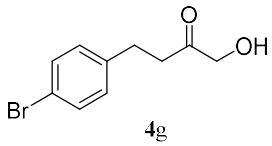 **4**g	13.762	D
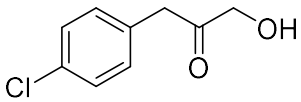 **4**b	8.113	C	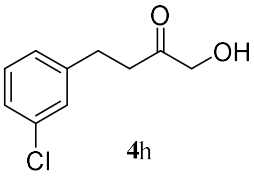 **4**h	9.061	D
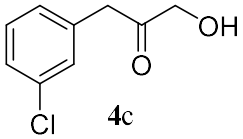 **4**c	7.907	C	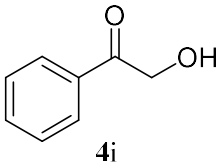 **4**i	4.627	B
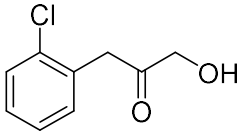 **4**d	6.909	C	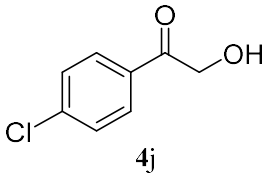 **4**j	5.570	C
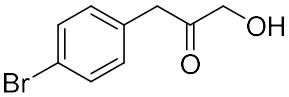 **4**e	5.537	C	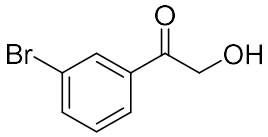 **4**k	5.913	D
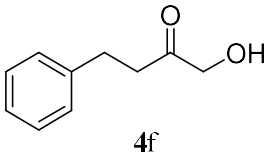 **4**f	5.455	C	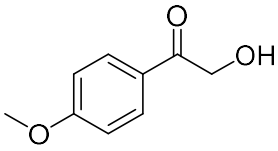 **4**l	8.320	C

Table S5. E-factor calculation.[a]

This work[b]					**Literature reported** [17][c]		
	(*S*)-**5**a		(*R*)-**5**a				
	Waste	E-Factor (g g^{-1})	Waste	E-Factor (g g^{-1})		Waste	E-Factor (g g^{-1})
Reaction	β-phenylethanol	0.01	β-phenylethanol	0.01	Reaction	L-Phe	0.09
	HCHO	0.19	HCHO	0.17		THF	30.14
	$MgSO_4$	0.16	$MgSO_4$	0.14		CH_3OH	26.78
	ThDP	0.08	ThDP	0.07		LiCl	0.92
	(*R*)-PEA	0.06	L-Ala	10.11		$NaBH_4$	0.82
	Acetophenone	0.10	Pyruvate	6.66		Amberlyst-15	16.95
	PLP	0.01	PLP	0.01		$NaHCO_3$	3.39
	Cells	23.40	Cells	20.34		NaCl	10.17
	DMSO	30.35	DMSO	26.01			
Extraction	EtOAc (95% recycle)	74.66	EtOAc (95% recycle)	64.00	Extraction	CH_2Cl_2	67.63
Total	129.02		127.52		Total	156.89	

[a]E-factor = (amount of total waste) [g] / (amount of product) [g]; [b]E-factors were calculated including solvents used and excluding water. [c]E-factors were calculated using the values in the respective literature, including solvents used and excluding water.

Table S6. EcoScale calculation.[18]

This work[b]		**Literature reported [17][c]**	
Parameter	Penalty	Parameter	Penalty
1 Yield: 60.0%	20	1 Yield: 92.0%	4
2 $MgSO_4$ (3.5 mmol)	0	2 $NaBH_4$ (32.6 mmol)	0
HCHO (27.6 mmol)	0	LiCl (32.6 mmol)	0
ThDP (0.4 mmol)	0	Amberlyst-15 (81.5 mmol)	0
DMSO	0	THF	0
		CH_3OH	0
3 Safety	0	3 $NaBH_4$ (T, F, E)	20
HCHO (T)	5	THF (T, F, E)	20
		MeOH (T, F)	10
		LiCl (T)	5
4 Common glassware, oscillation	0	4 Common glassware, stirring and reflux	0
5 Room temperature, 15 h	1	5 Room temperature, <24h	1
6 Liquid-liquid extraction	3	6 Removal of THF by decantation	0
Removal of EtOAc	0	Liquid-liquid extraction	3
Silica gel chromatography	10	Washing with brine	3
		Removal of CH_2Cl_2	0
		Crystallization	1
Penalty points total	39	Penalty points total	67
EcoScale	**61**	**EcoScale**	**33**

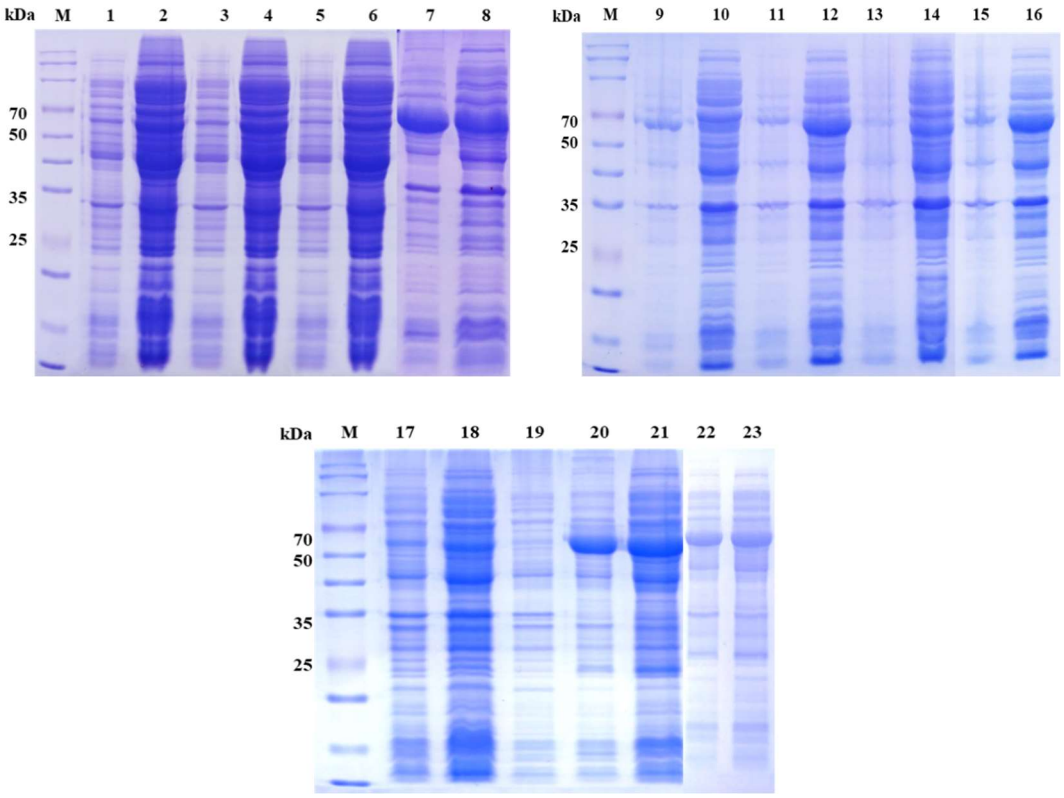

Figure S1. SDS-PAGE of *E. coli* (BALs). Lane M: protein marker; Lane 1-2: BrBAL (61.25kDA); Lane 3-4: DeBAL (61.55kDA); Lane 5-6: AgBAL (61.20kDA); Lane 7-8: RpBAL (60.30kDA); Lane 9-10: RbBAL (61.51kDA); Lane 11-12: RhBAL (61.70kDA); Lane 13-14: MeBAL (60.43kDA); Lane 15-16: CsBAL (59.90kDA); Lane 17-18: AbBAL (60.14kDA); Lane 20-21: PaBAL (59.54kDA); Lane 22-23: CnBAL (59.86kDA); Lane 1, 3, 5, 7, 9, 11, 13, 15, 17, 20, 22: cell-free extracts of recombinant *E. coli* (BALs); Lane :2, 4, 6, 8, 10, 12, 14, 16, 18, 21, 23: *E. coli* (BALs) resting cells; Lane 19: resting cells of *E. coli* (pET28a) with empty plasmid.

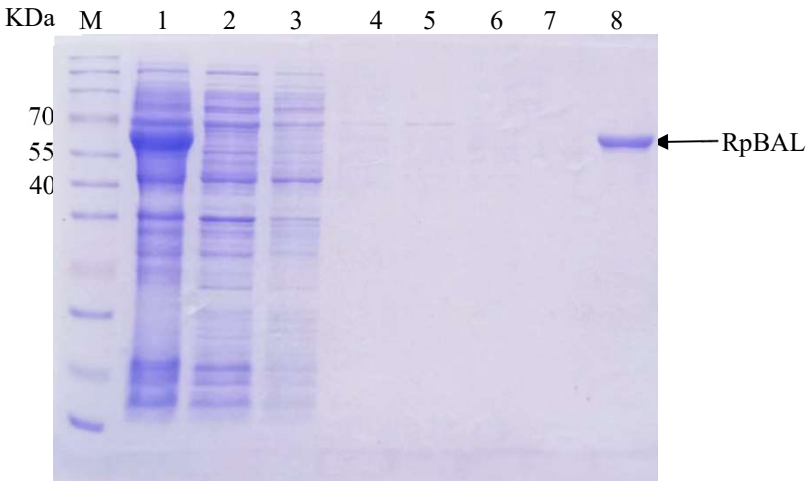

Figure S2. SDS-PAGE analysis of RpBAL. Lane M: marker; Lane 1: cell-free extract of *E. coli* (RpBAL); Lane 2: flow-through solution; Lane 3: equilibration solution; Lane 4: fraction washed with 20 mM imidazole; Lane 5: fraction washed with 50 mM imidazole; Lane 6: fraction washed with 100 mM imidazole; Lane 7: fraction washed with 250 mM imidazole. Lane 8: fraction (purified RpBAL) washed with 500 mM imidazole (about 60 kDa).

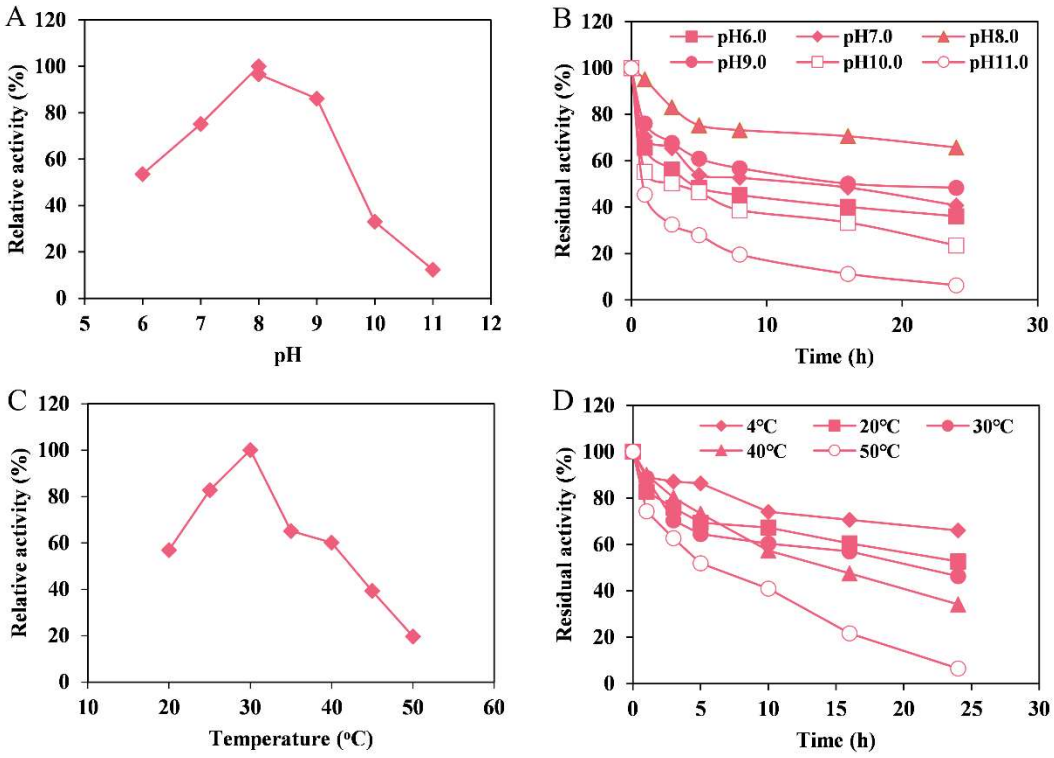

Figure S3. The effect of pH and temperature on the activity and stability of RpBAL.

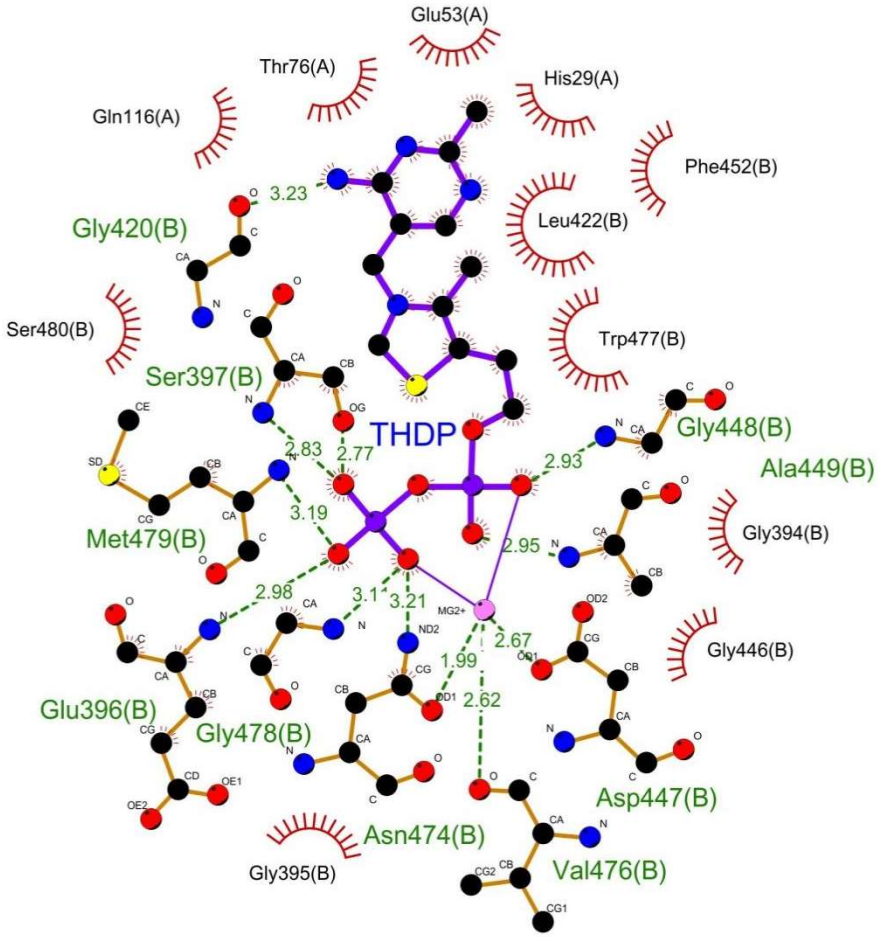

Figure S4. The ThDP and its interaction with RpBAL. Distance are illustrate in angstrom.

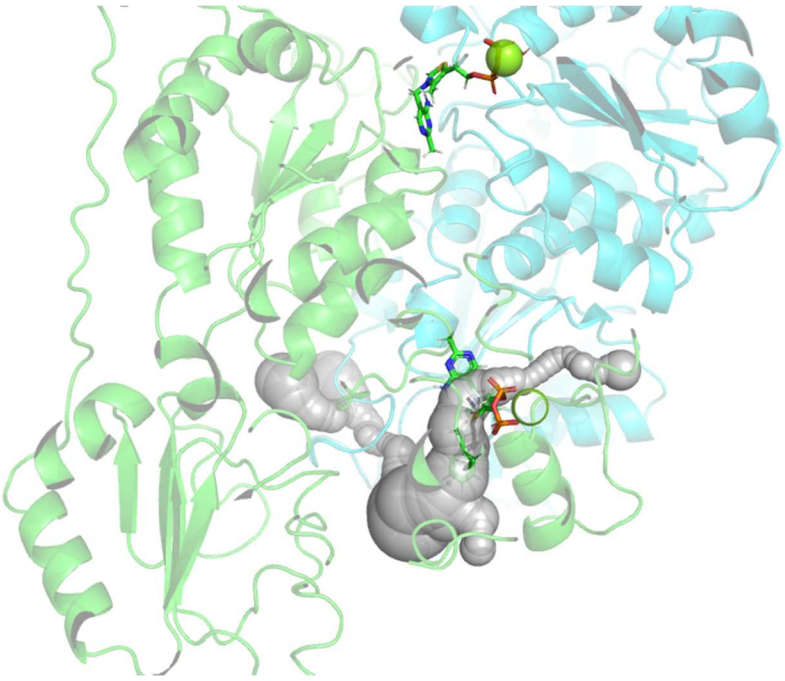

Figure S5. The tunnel of PfBAL.

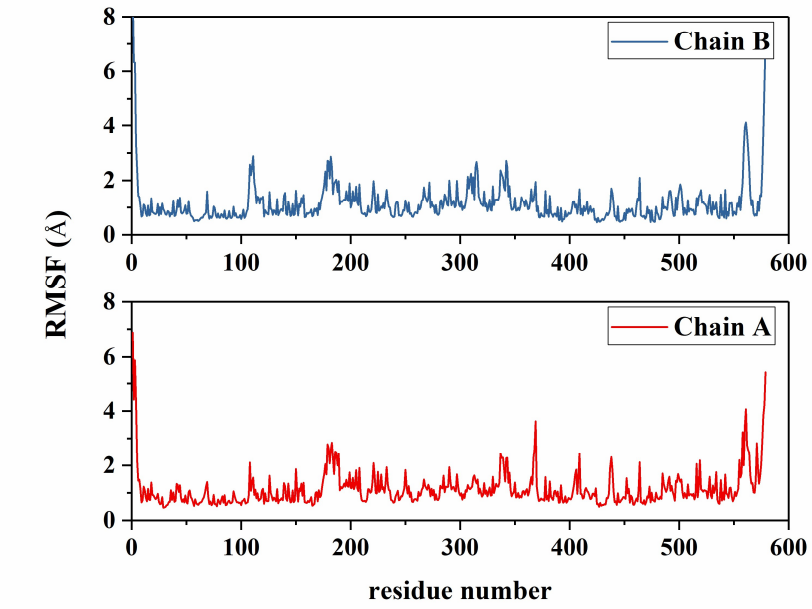

Figure S6. The RMSF of RpBAL. Distances are illustrated in angstrom.

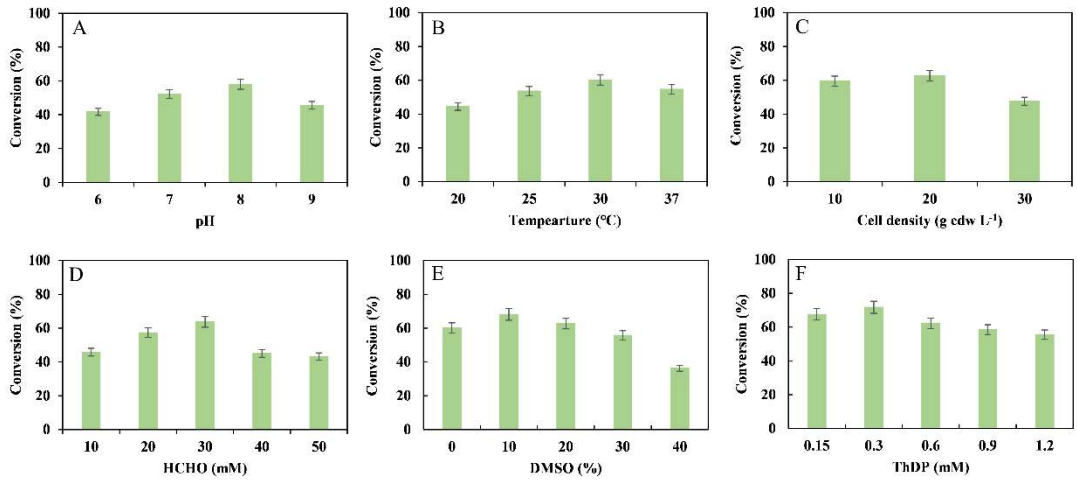

Figure S7. Optimization of reaction conditions for conversion of **3**a to **4**a with the resting cells of *E. coli* (RpBAL). (A) pH; (B) temperature; (C) cell density; (D) HCHO concentration; (E) DMSO concentration; (F) ThDP concentration.

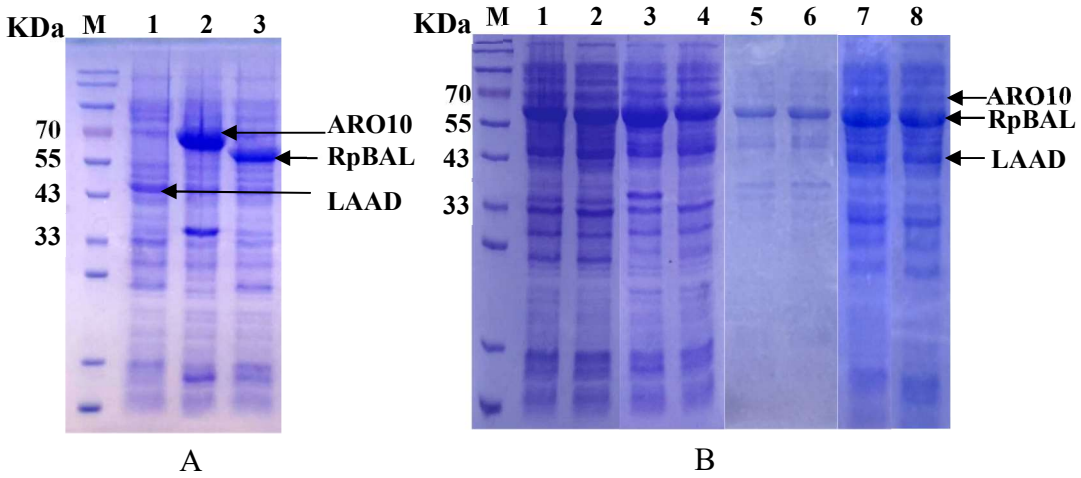

Figure S8. SDS-PAGE of recombinant *E. coli* cells and co-expression of multiple enzymes. **A**: Lane M: protein marker; Lane 1: *E. coli* (LAAD); Lane 2: *E. coli* (ARO10); Lane 3: *E. coli* (RpBAL); **B**: Lane M: protein marker; Lane 1: *E. coli* (EAR-CL), Lane 2: *E. coli* (EAL-RR), Lane 3: *E. coli* (RRL-EA), Lane 4: *E. coli* (RRL-CA), Lane 5: *E. coli* (CRL-EA), Lane 6: *E. coli* (CRL-RA), Lane 7: *E. coli* (EA-CL-RR) Lane 8: *E. coli* (EL-CA-RR).

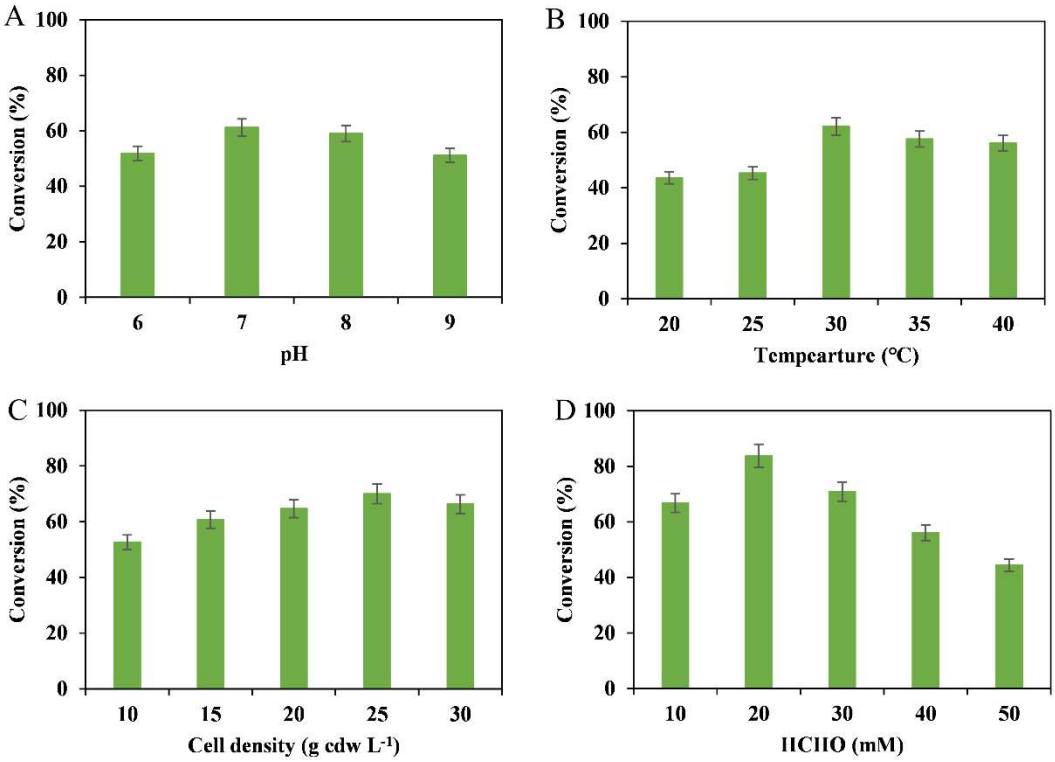

Figure S9. Optimization of the reaction conditions for the conversion of **1**a to **4**a with the resting cells of *E. coli* (EAL-RR). (A) pH; (B) temperature; (C) cell density; (D) HCHO concentration.

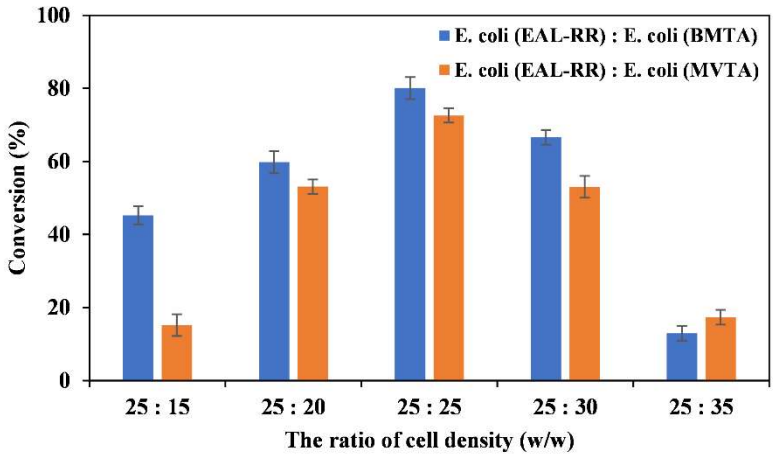

Figure S10. Optimization of cell density ratio for converting **1**a to **5**a.

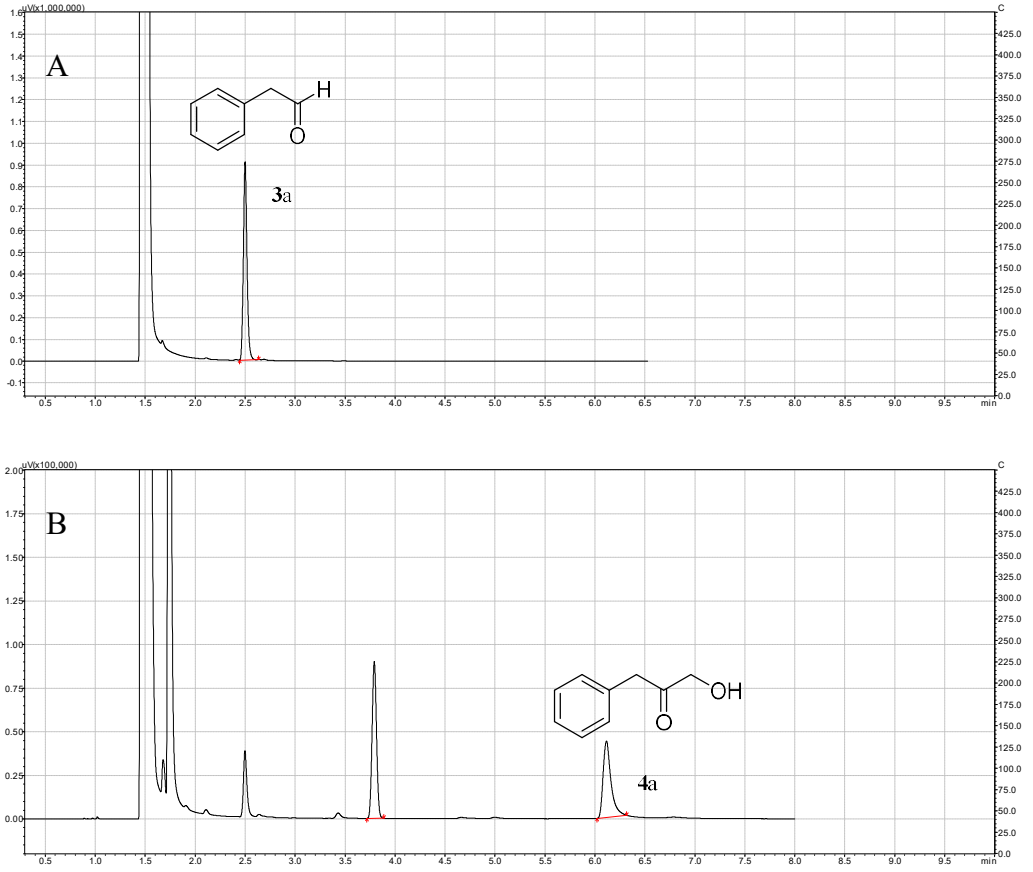

Figure S11. GC analysis of 1-hydroxy-3-phenylpropan-2-one **4**a. A: phenylacetaldehyde **3**a standard; B: 1-hydroxy-3-phenylpropan-2-one **4**a produced from phenylacetaldehyde **3**a (10 mM) with 20 g CDW/L of *E. coli* (RpBAL) at 6 h.

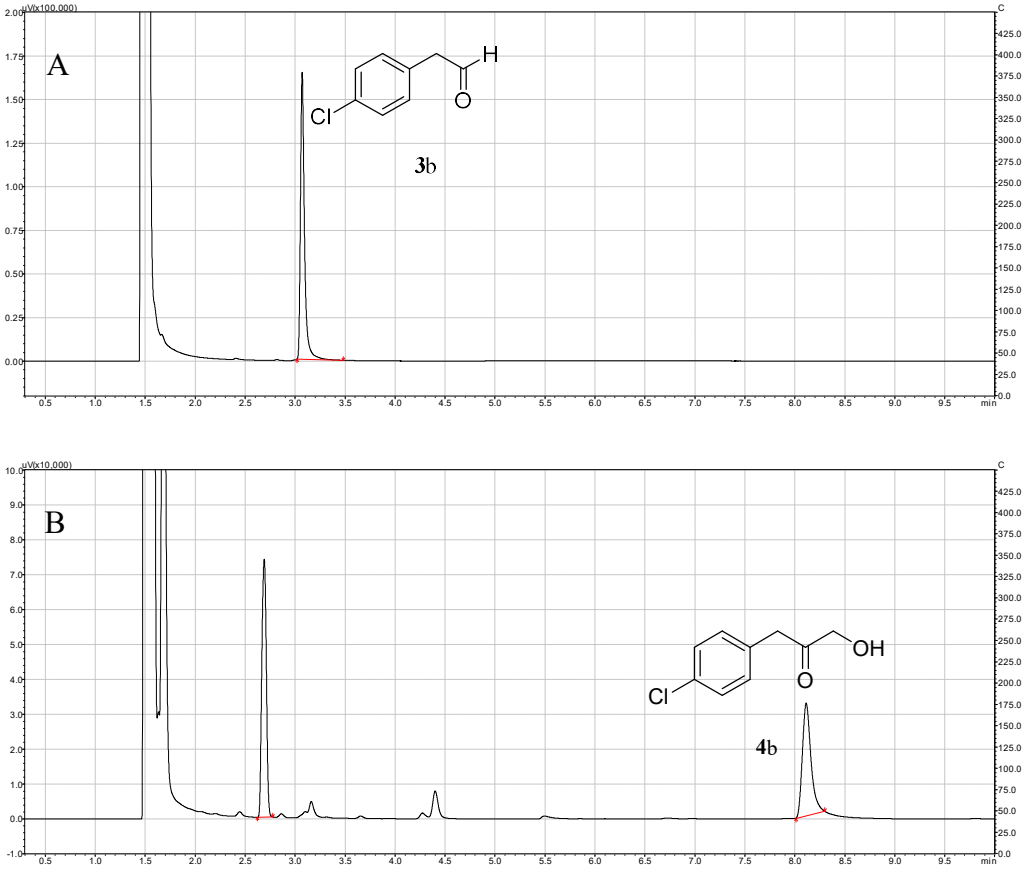

Figure S12. GC analysis of 1-(4-chlorophenyl)-3-hydroxy-2-propanone **4**b. A: 4-chlorobenzeneacetaldehyde **3**b standard; B: 1-(4-chlorophenyl)-3-hydroxy-2-propanone **4**b produced from 4-chlorobenzeneacetaldehyde **3**b (10 mM) with 20 g CDW/L of *E. coli* (RpBAL) at 4 h.

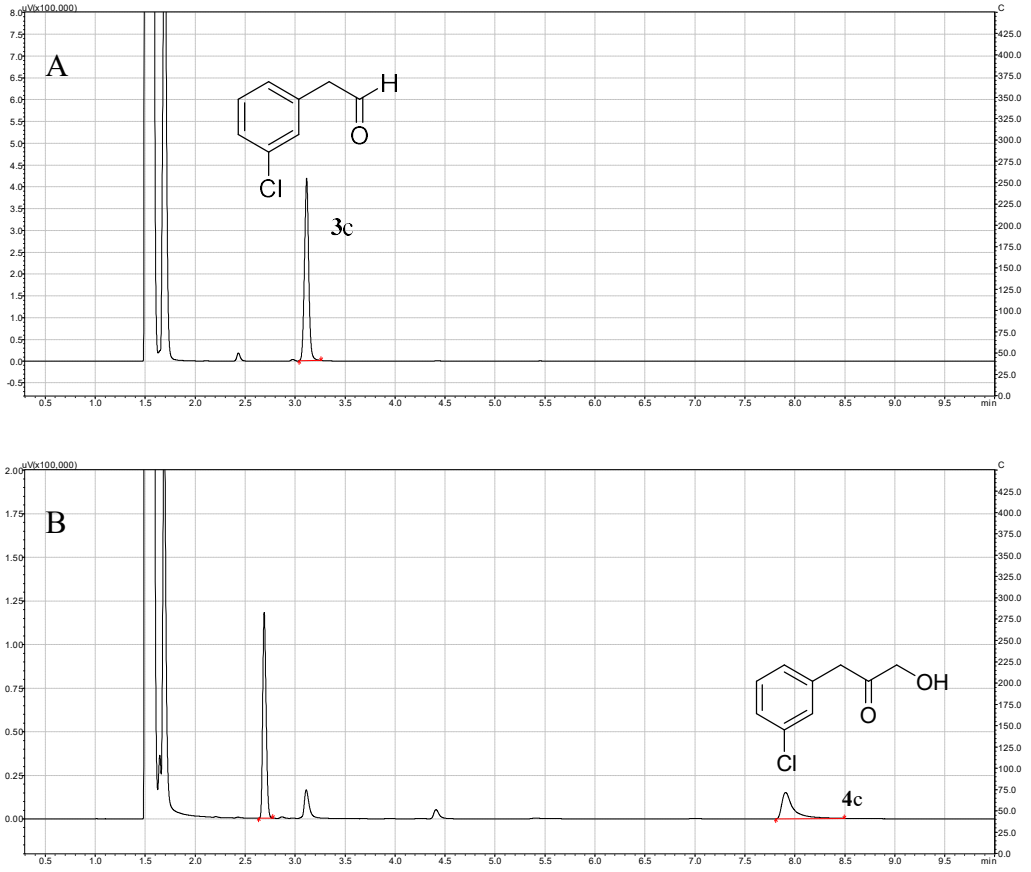

Figure S13. GC analysis of 1-(3-chlorophenyl)-3-hydroxy-2-propanone **4**c. A: 3-chlorobenzeneacetaldehyde **3**c standard; B: 1-(3-chlorophenyl)-3-hydroxy-2-propanone **4**c produced from 3-chlorobenzeneacetaldehyde **3**c (10 mM) with 20 g CDW/L of *E. coli* (RpBAL) at 10 h.

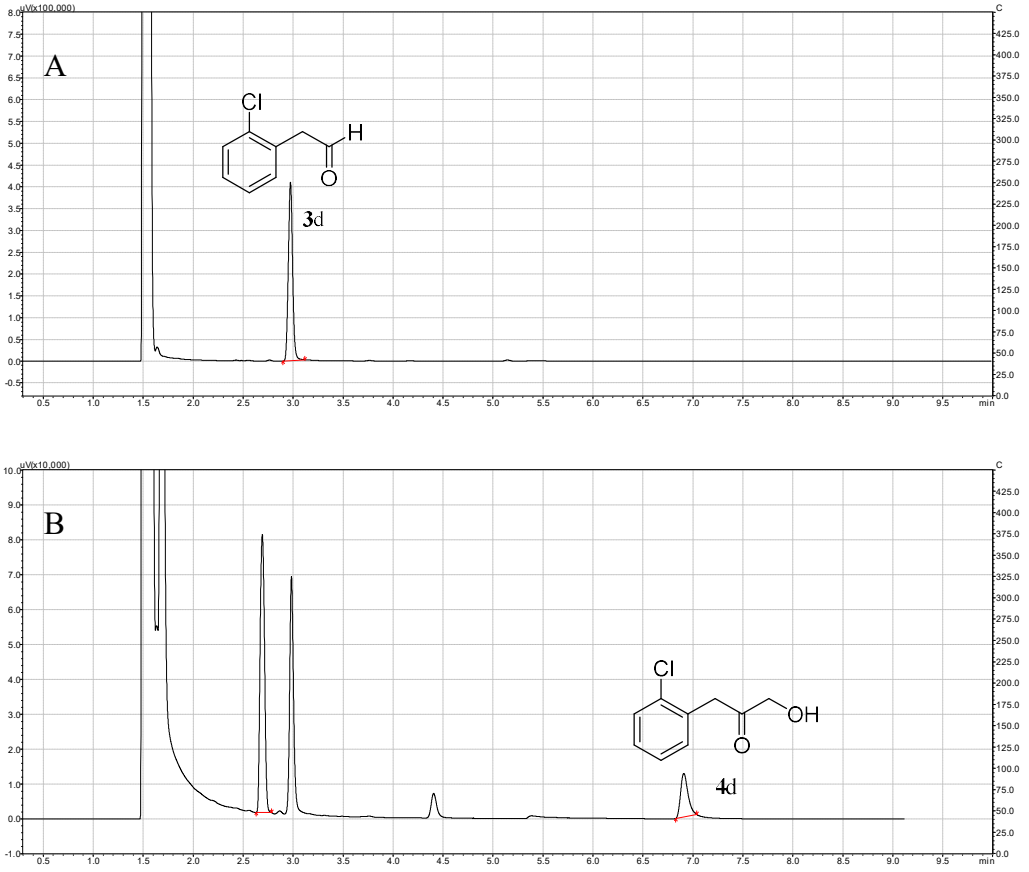

Figure S14. GC analysis of 1-(2-chlorophenyl)-3-hydroxy-2-propanone **4**d. A: 2-chlorobenzeneacetaldehyde **3**d standard; B: 1-(2-chlorophenyl)-3-hydroxy-2-propanone **4**d produced from 2-chlorobenzeneacetaldehyde **3**d (10 mM) with 20 g CDW/L of *E. coli* (RpBAL) at 10 h.

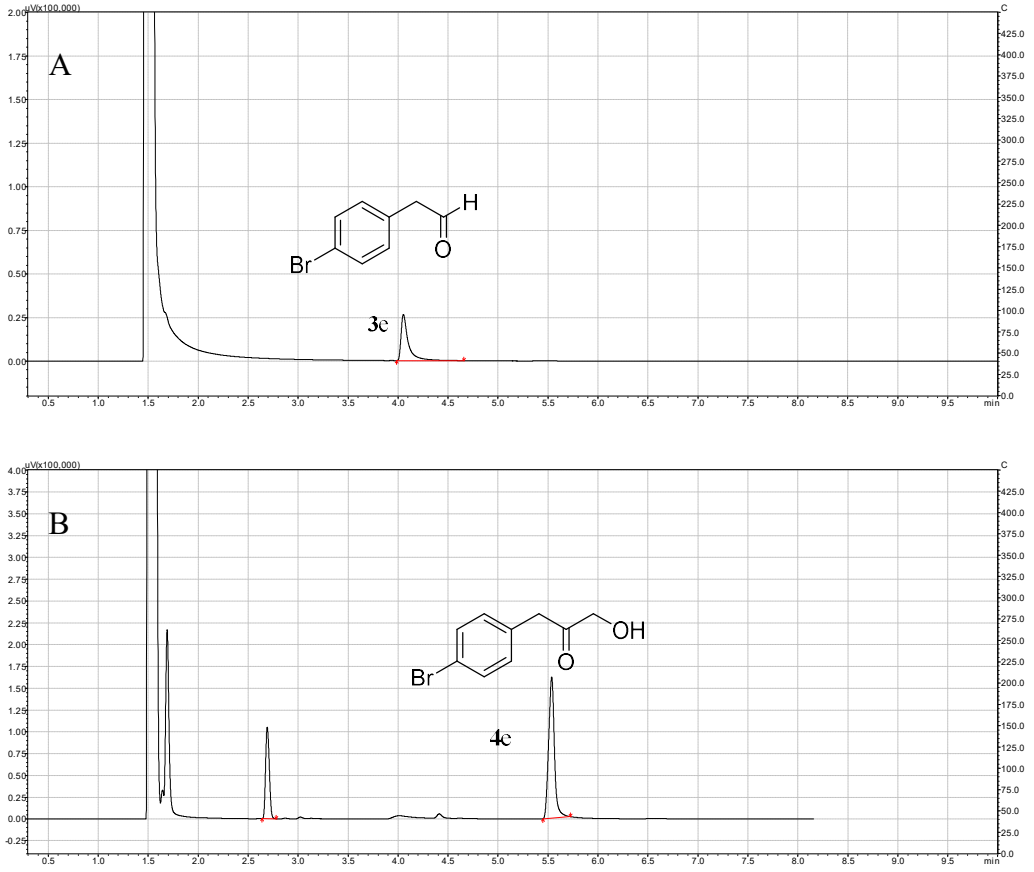

Figure S15. GC analysis of 1-(4-bromophenyl)-3-hydroxy-2-propanone **4**e. A: 4-bromobenzeneacetaldehyde **3**e standard; B: 1-(4-bromophenyl)-3-hydroxy-2-propanone **4**e produced from 4-bromobenzeneacetaldehyde **3**e (10 mM) with 20 g CDW/L of *E. coli* (RpBAL) at 4 h.

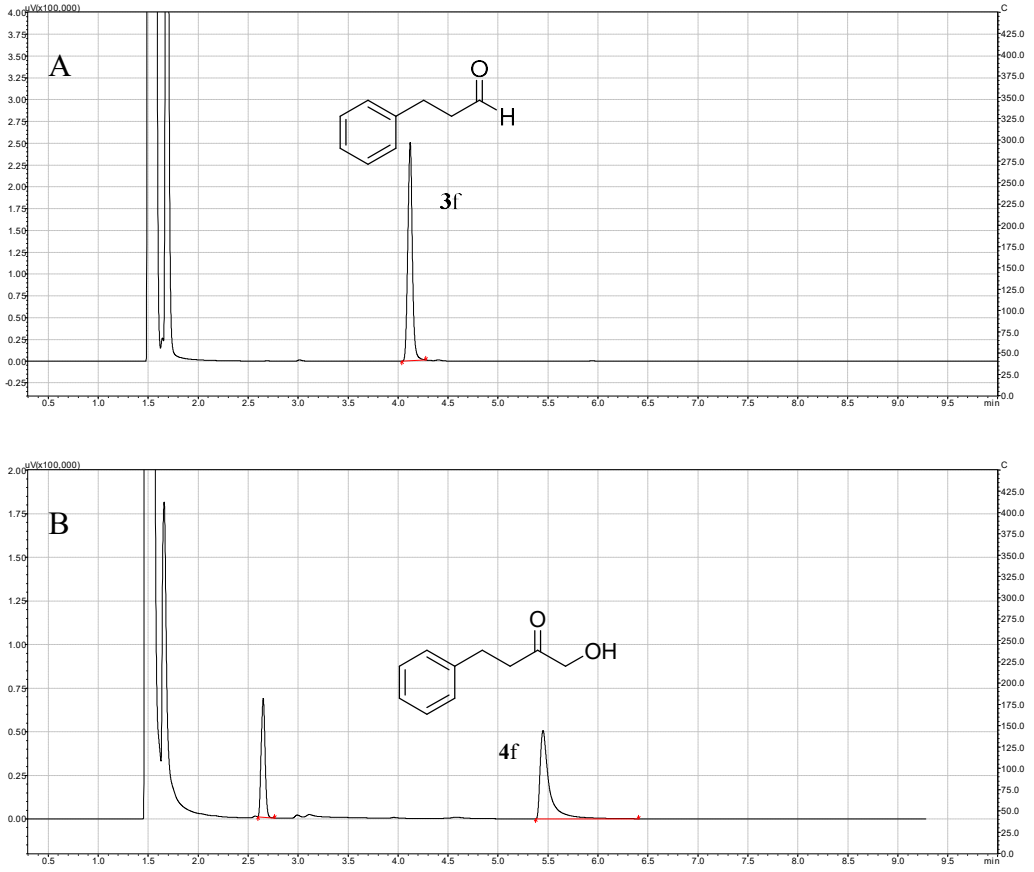

Figure S16. GC analysis of 1-hydroxy-4-phenyl-2-butanone **4**f. A: benzenepropanal **3**f standard; B: 1-hydroxy-4-phenyl-2-butanone **4**f produced from benzenepropanal **3**f (10 mM) with 20 g CDW/L of *E. coli* (RpBAL) at 24 h.

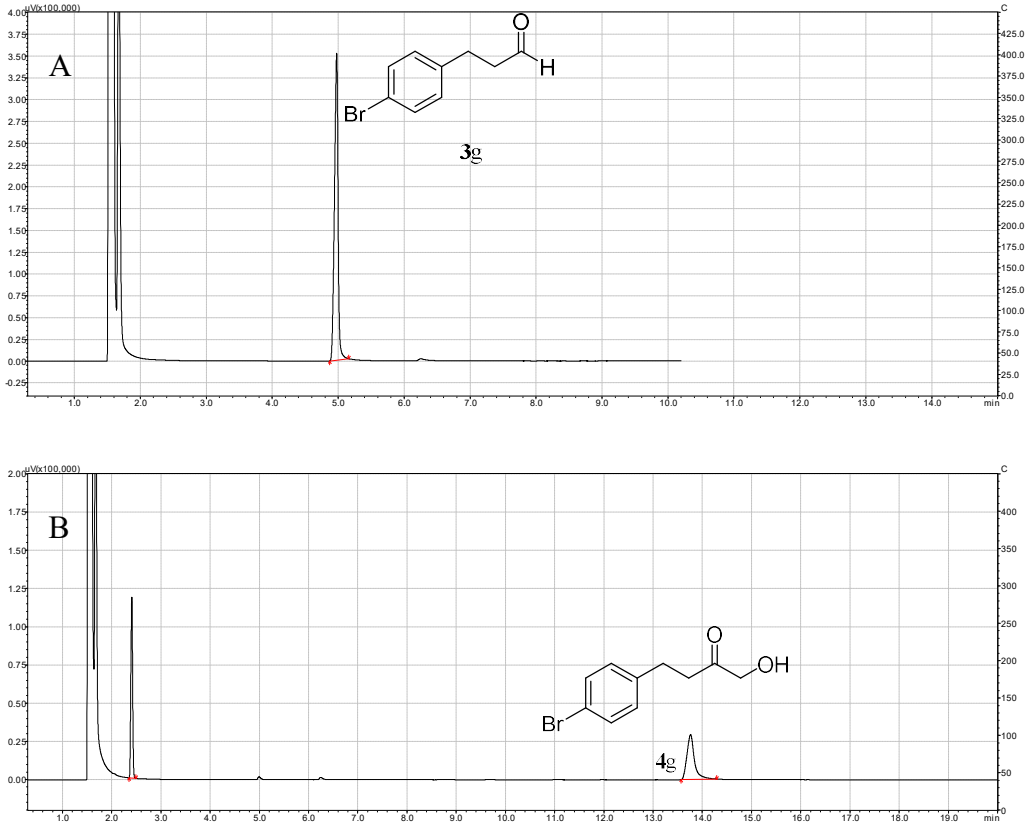

Figure S17. GC analysis of 4-(4-bromophenyl)-1-hydroxy-2-butanone **4**g. A: 3-(4-bromophenyl)propanal **3**g standard; B: 4-(4-bromophenyl)-1-hydroxy-2-butanone **4**g produced from 3-(4-bromophenyl)propanal **3**g (10 mM) with 20 g CDW/L of *E. coli* (RpBAL) at 9 h.

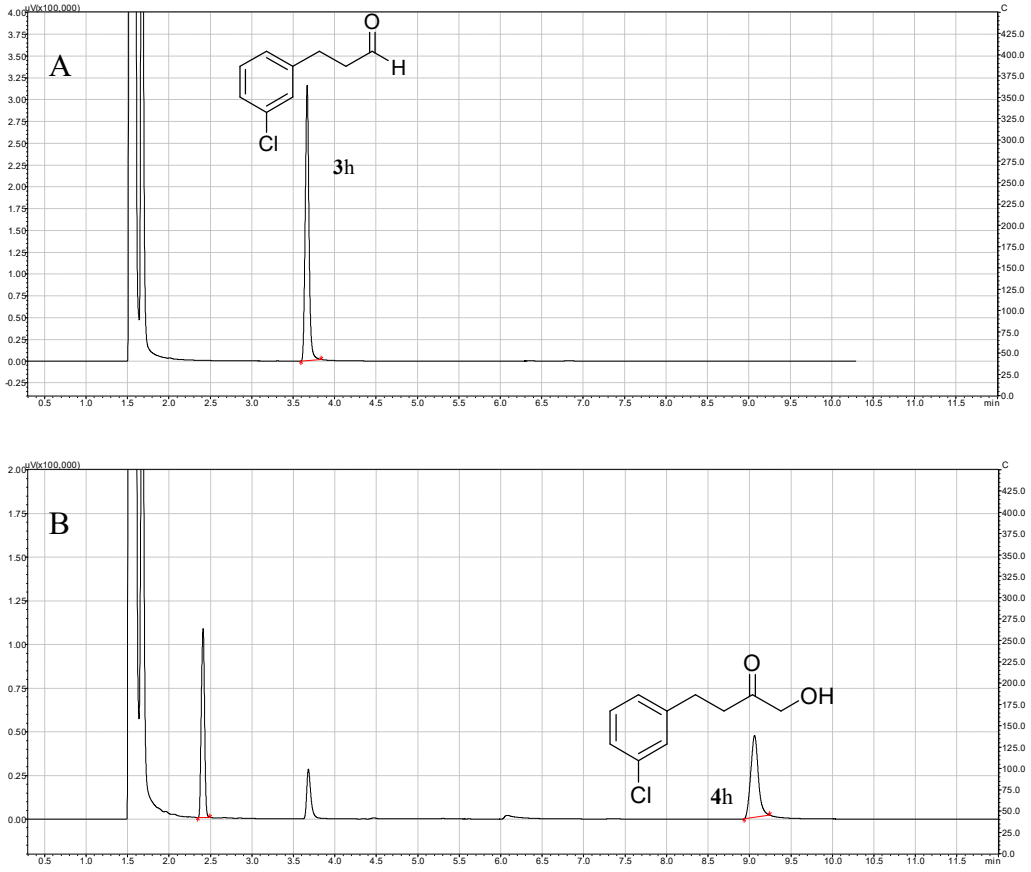

Figure S18. GC analysis of 4-(3-chlorophenyl)-1-hydroxy-2-butanone **4**h. A: 3-(3-chlorophenyl)propionaldehyde **3**h standard; B: 4-(3-chlorophenyl)-1-hydroxy-2-butanone **4**h produced from 3-(3-chlorophenyl)propionaldehyde **3**h (10 mM) with 20 g CDW/L of *E. coli* (RpBAL) at 24 h.

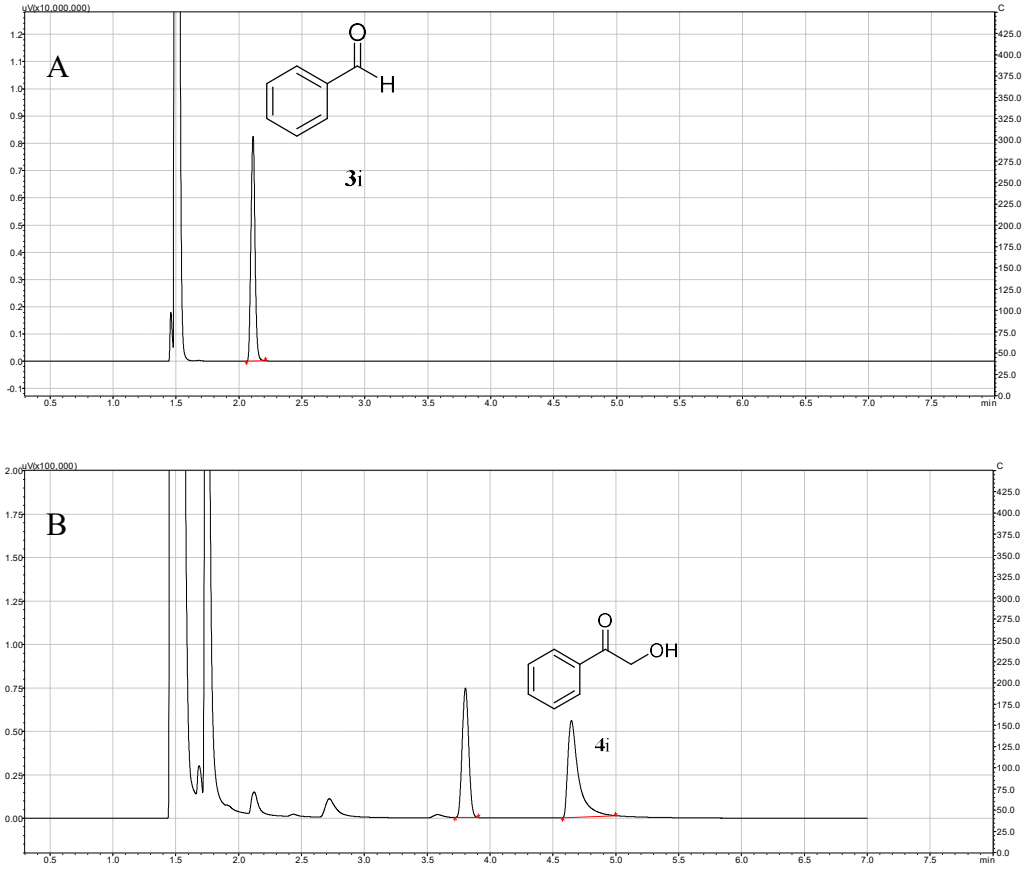

Figure S19. GC analysis of 2-hydroxyacetophenone **4**i. A: benzaldehyde **3**i standard; B: 2-hydroxyacetophenone **4**i produced from benzaldehyde **3**i (10 mM) with 20 g CDW/L of *E. coli* (RpBAL) at 4 h.

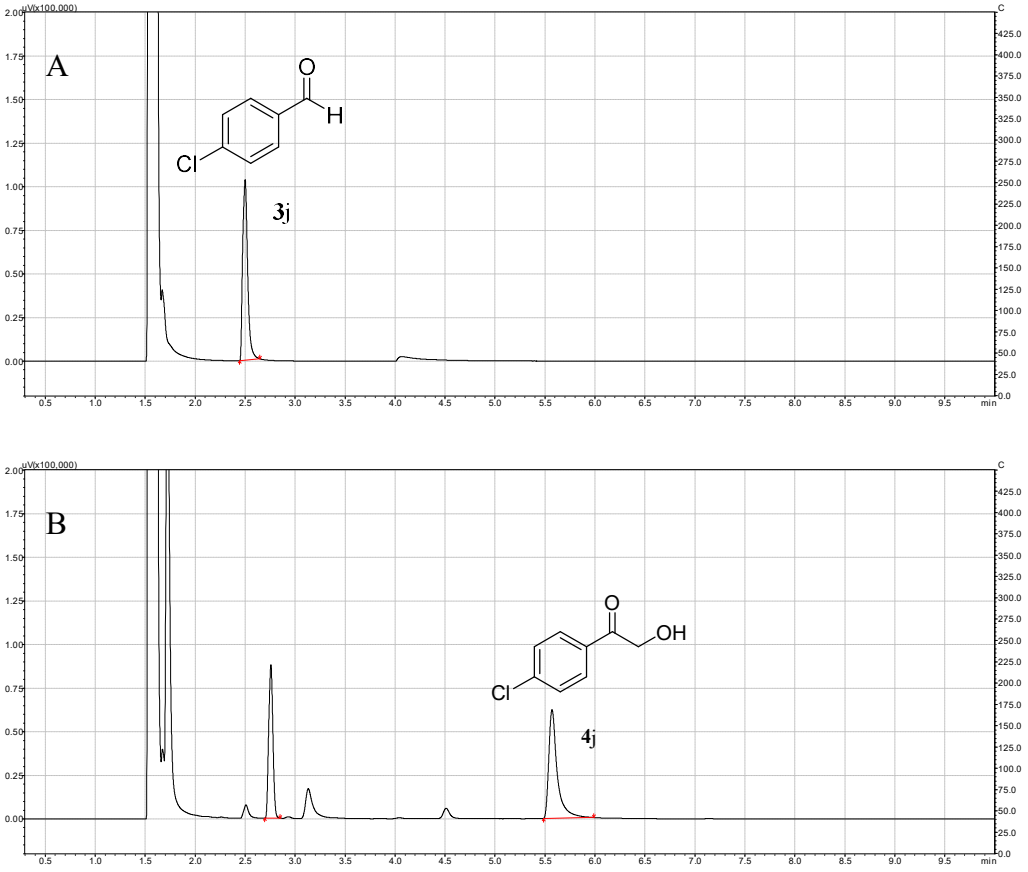

Figure S20. GC analysis of 1-(4-chlorophenyl)-2-hydroxyethanone **4**j. A: 4-chlorobenzaldehyde **3**j standard; B: 1-(4-chlorophenyl)-2-hydroxyethanone **4**j produced from 4-chlorobenzaldehyde **3**j (10 mM) with 20 g CDW/L of *E. coli* (RpBAL) at 4 h.

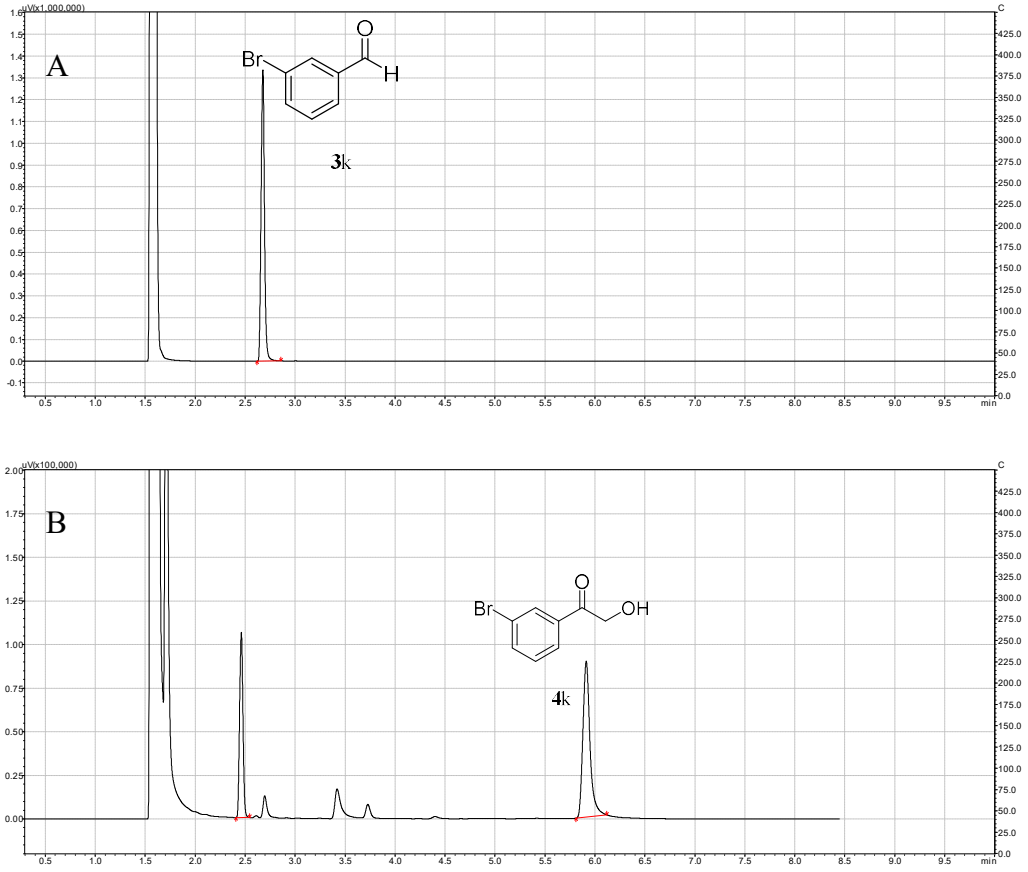

Figure S21. GC analysis of 1-(3-bromophenyl)-2-hydroxyethanone **4**k. A: 3-bromobenzaldehyde **3**k standard; B: 1-(3-bromophenyl)-2-hydroxyethanone **4**k produced from 3-bromobenzaldehyde **3**k (10 mM) with 20 g CDW/L of *E. coli* (RpBAL) at 4 h.

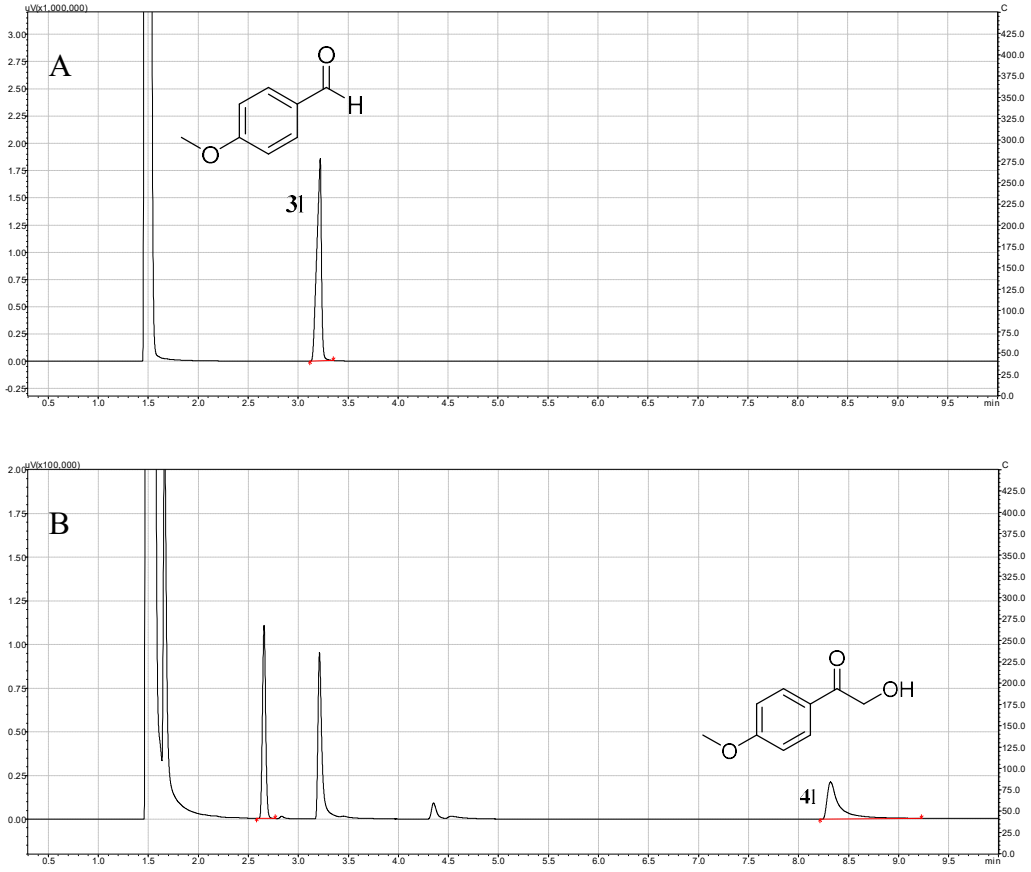

Figure S22. GC analysis of 2-hydroxy-1-(4-methoxyphenyl)ethanone **4**l. A: 4-methoxybenzaldehyde **3**l standard; B: 2-Hydroxy-1-(4-methoxyphenyl)ethanone **4**l produced from 4-methoxybenzaldehyde **3**l (10 mM) with 20 g CDW/L of *E. coli* (RpBAL) at 4 h.

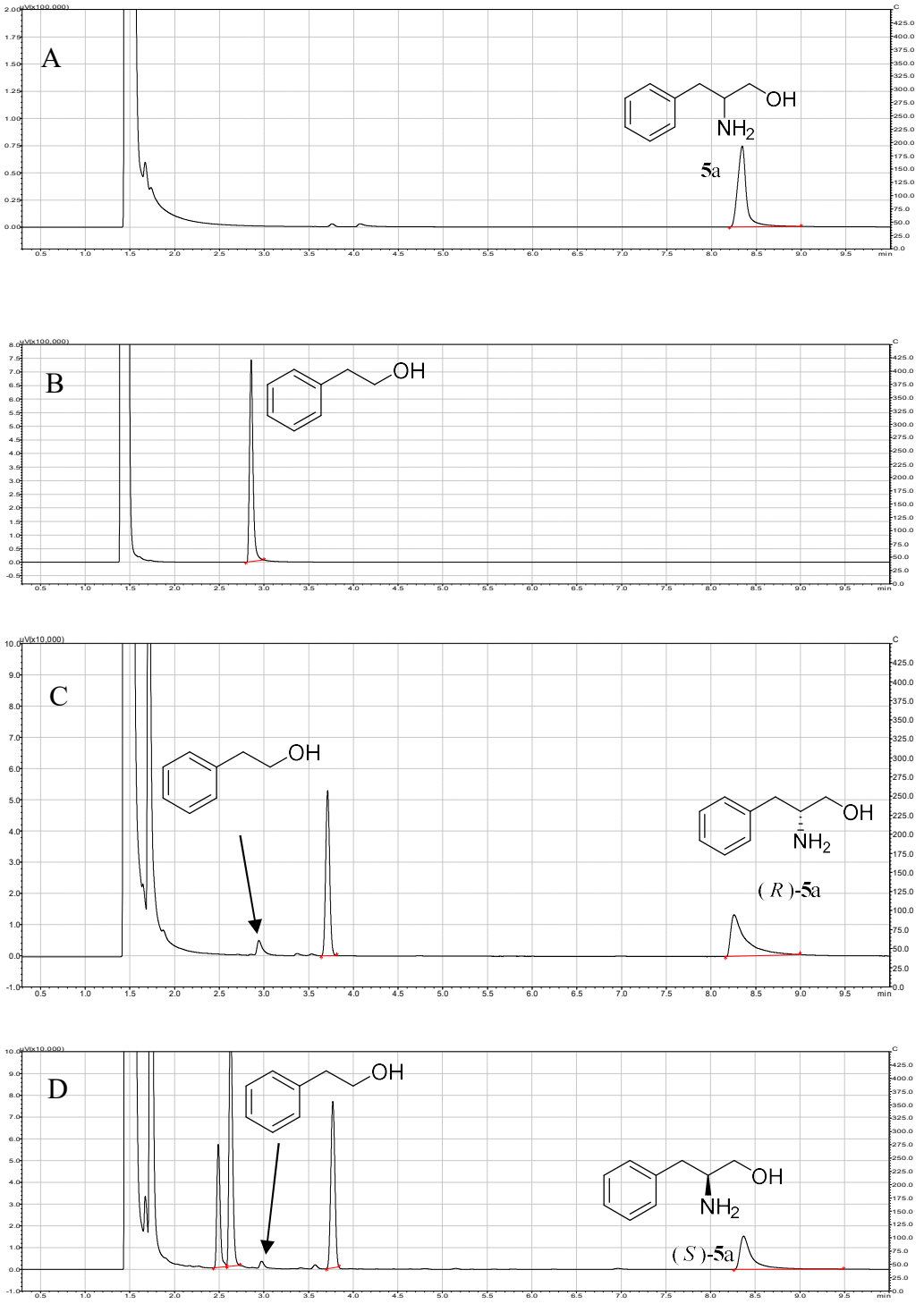

Figure S23. Achiral GC chromatograms of **5**a. A: **5**a standard. B: β-Phenylethanol standard. C: One-pot two-stage bioconversion of **1**a (10 mM) to **5**a with resting cells of *E. coli* (EAL-RR) and *E. coli* (BMTA) at 15 h. D: One-pot two-stage bioconversion of **1**a (10 mM) to **5**a with resting cells of *E. coli* (EAL-RR) and *E. coli* (MVTA) at 15 h.

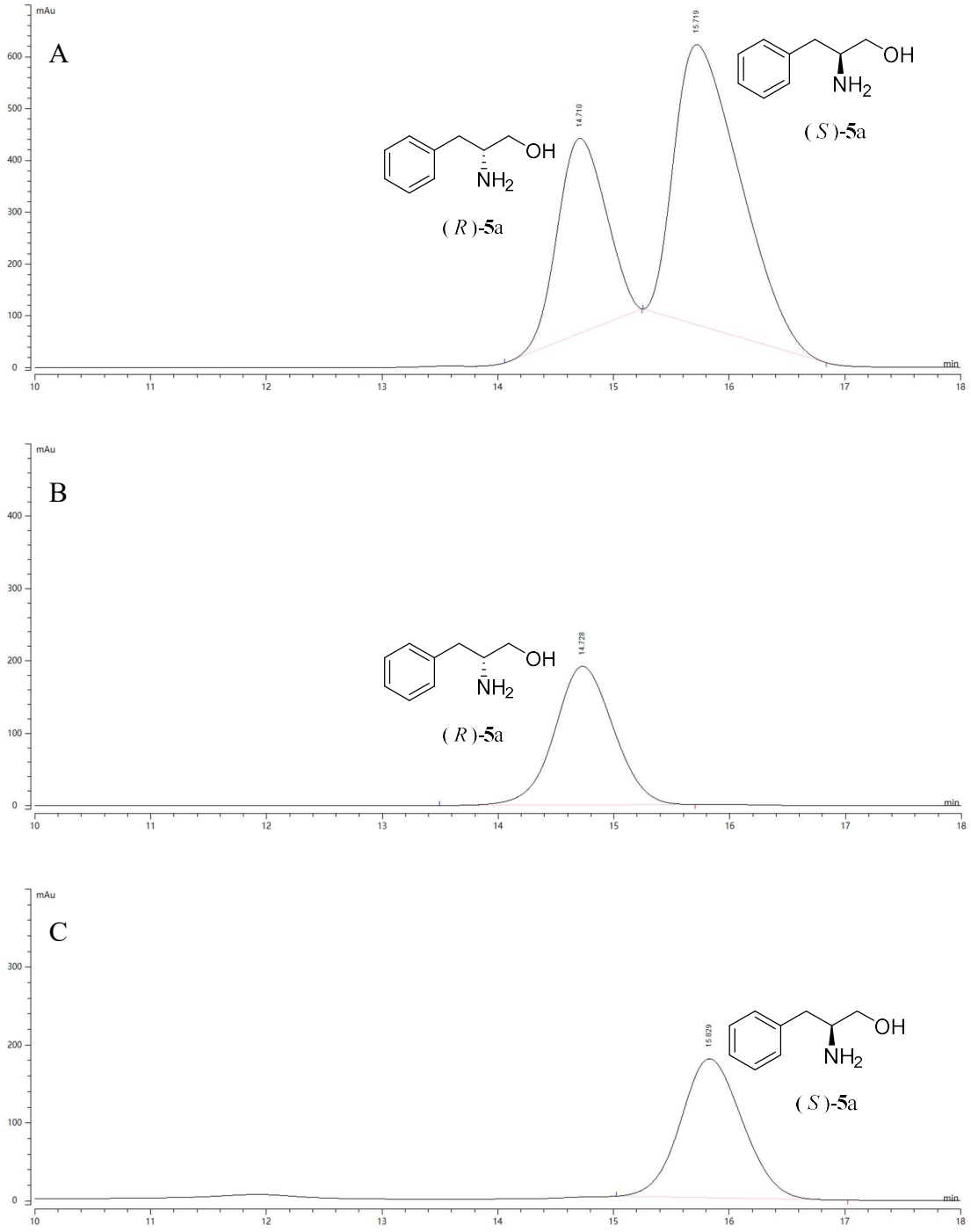

Figure S24. Chiral HPLC analysis of **5**a. A: (±)- **5**a standard. B: (*R*)-**5**a produced by conversion of **1**a (10 mM) with resting cells of *E. coli* (EAL-RR) and *E. coli* (BMTA) at 15 h. C: (*S*)-**5**a produced by conversion of **1**a (10 mM) with resting cells of *E. coli* (EAL-RR) and *E. coli* (MVTA) at 15 h.

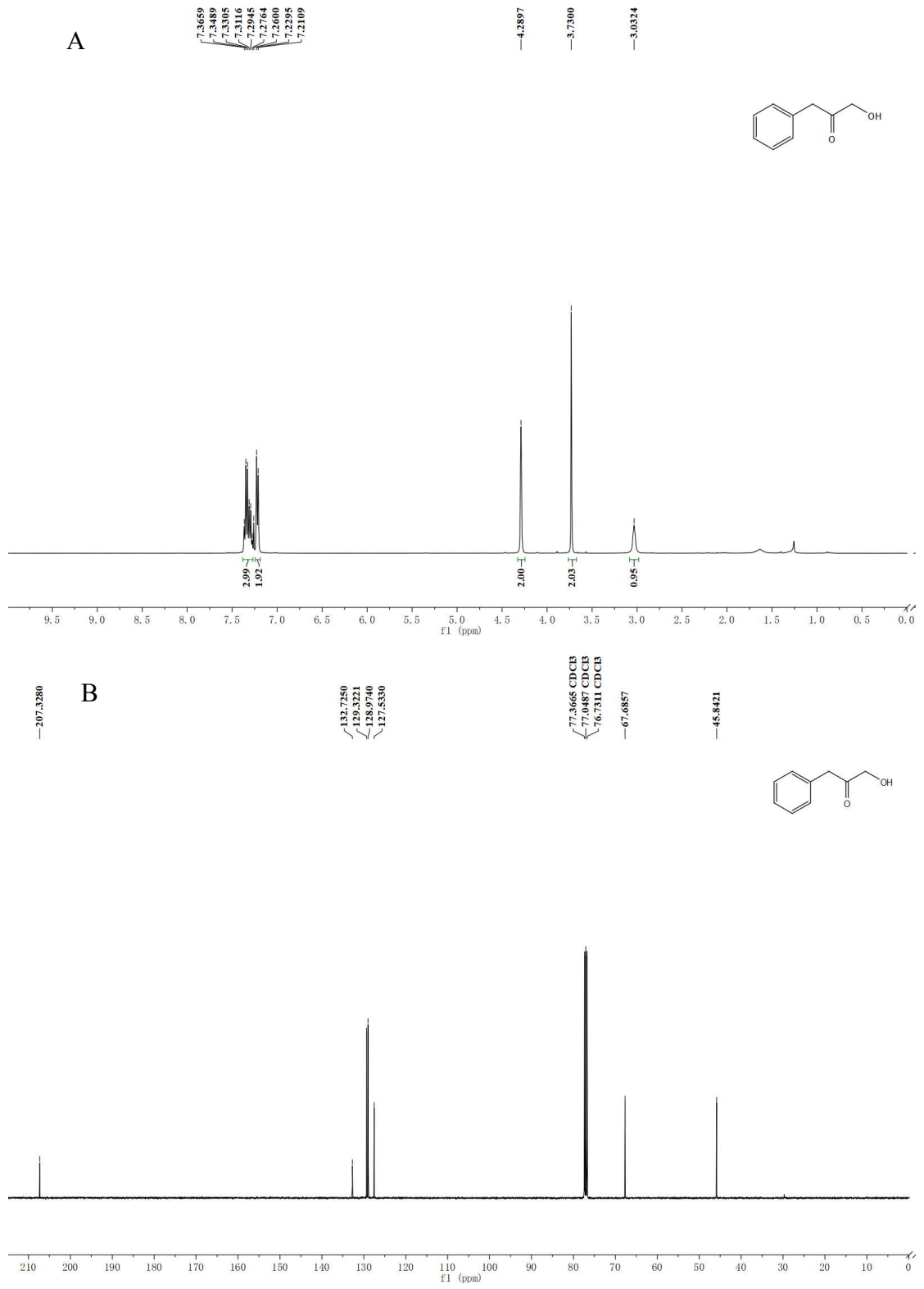

Figure S25. NMR spectra of 1-hydroxy-3-phenylpropan-2-one **4**a. A: ^{1}H-NMR spectra of **4**a; B: ^{13}C-NMR spectra of **4**a.

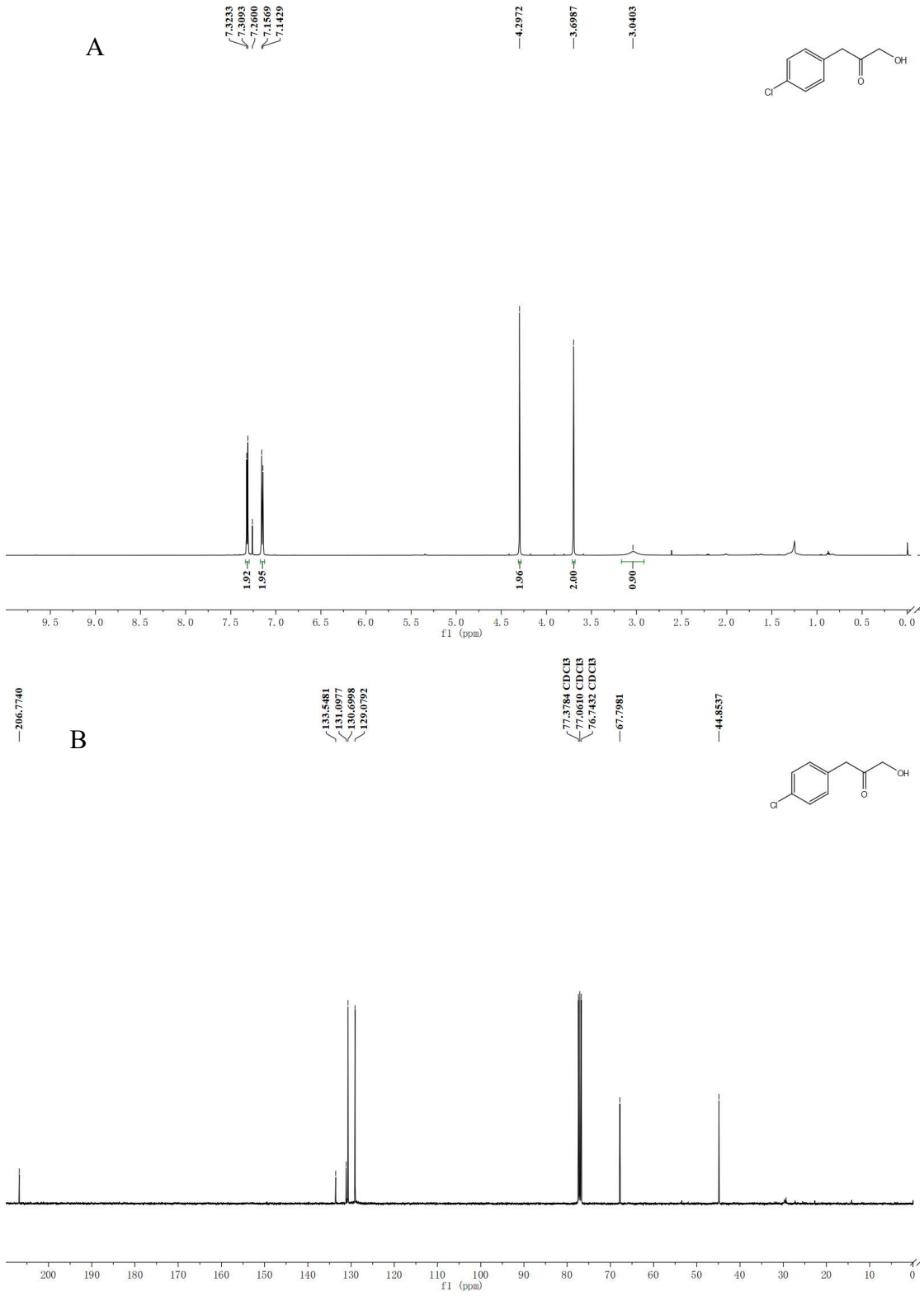

Figure S26. NMR spectra of 1-(4-chlorophenyl)-3-hydroxy-2-propanone **4**b. A: ^{1}H-NMR spectra of **4**b.

B: ^{13}C-NMR spectra of **4**b.

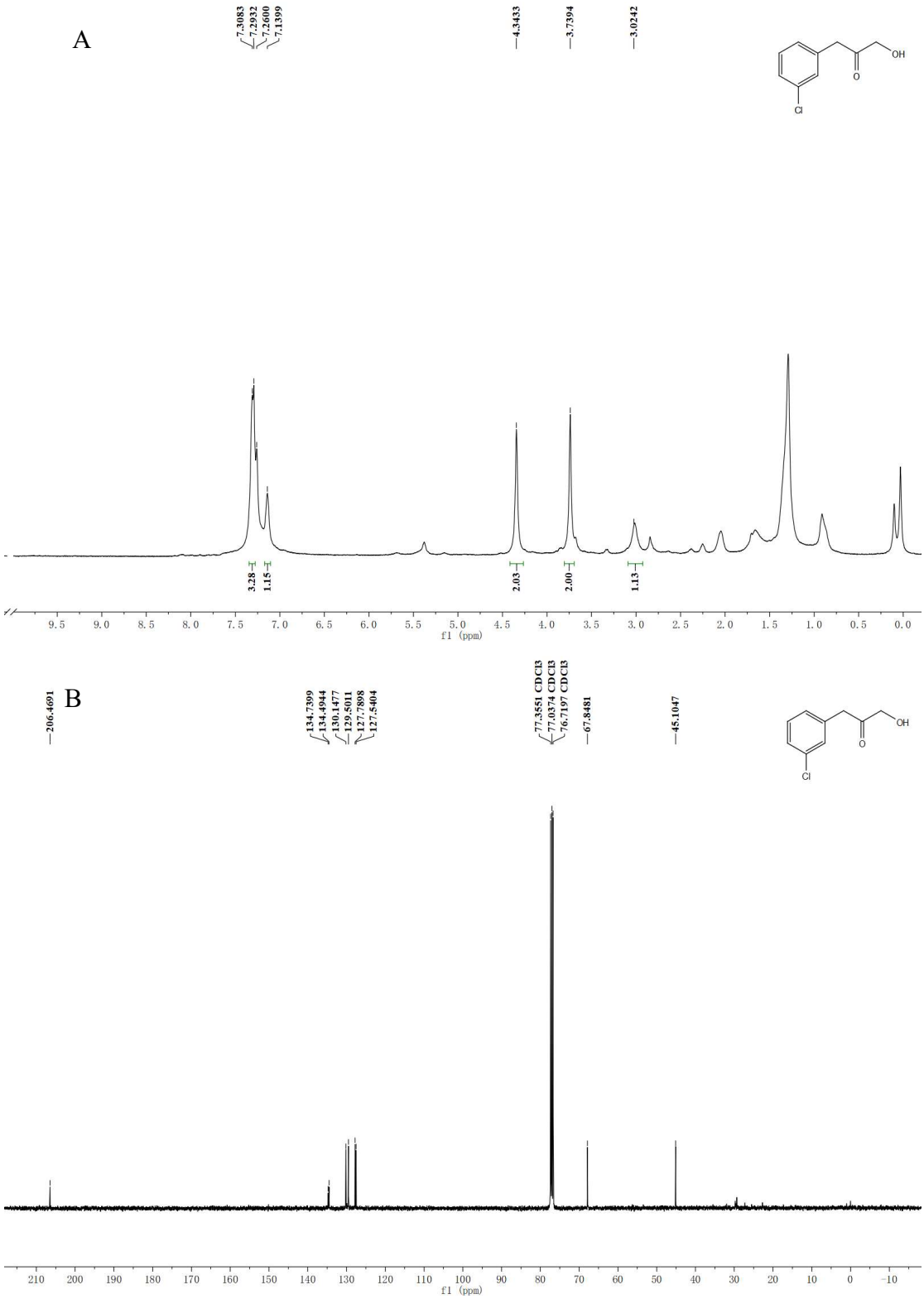

Figure S27. NMR spectra of 1-(3-chlorophenyl)-3-hydroxy-2-propanone **4**c. A: ^{1}H-NMR spectra of **4**c; B: ^{13}C-NMR spectra of **4**c.

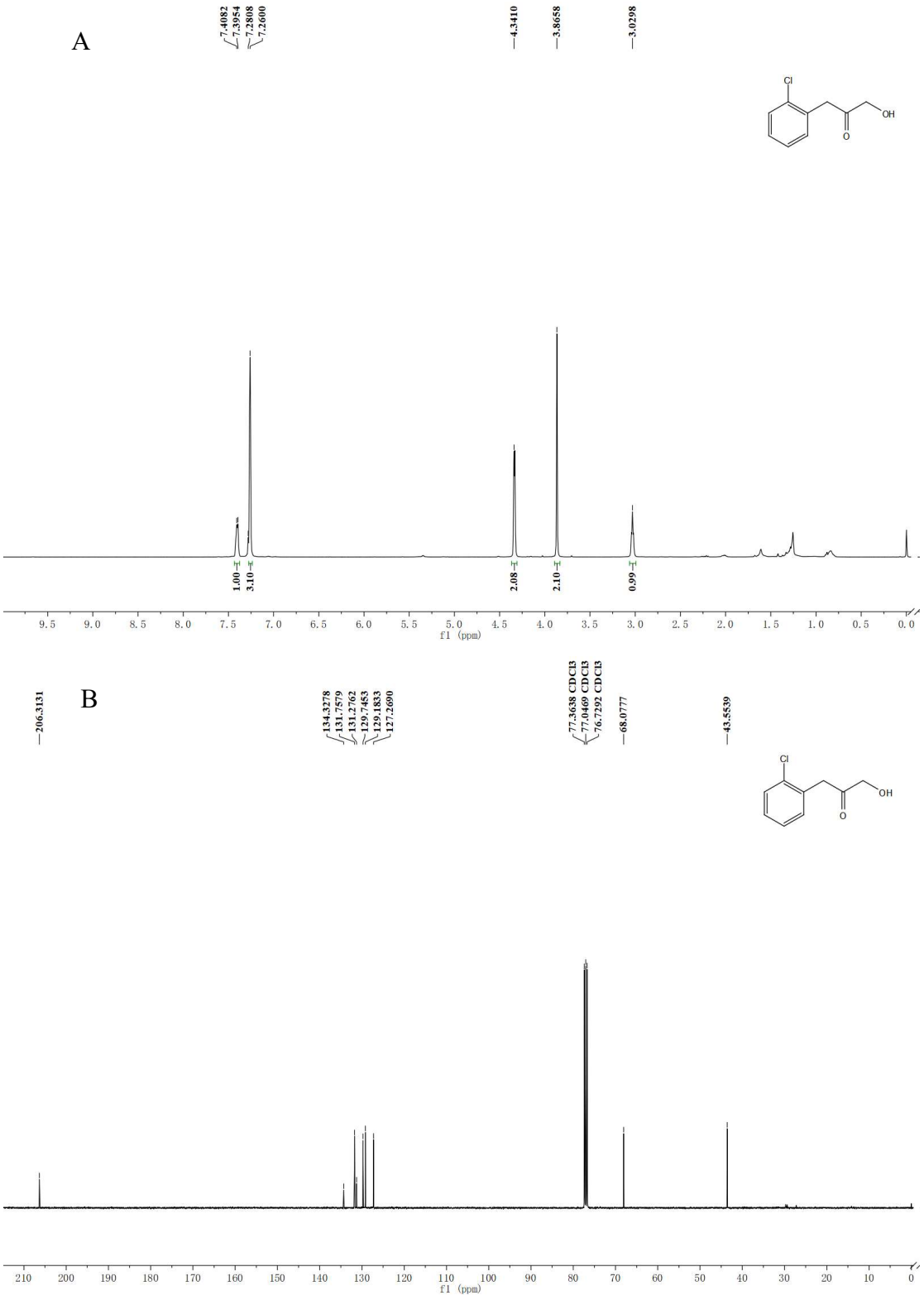

Figure S28. NMR spectra of 1-(2-chlorophenyl)-3-hydroxy-2-propanone **4**d. A: ^{1}H-NMR spectra of **4**d; B: ^{13}C-NMR spectra of **4**d.

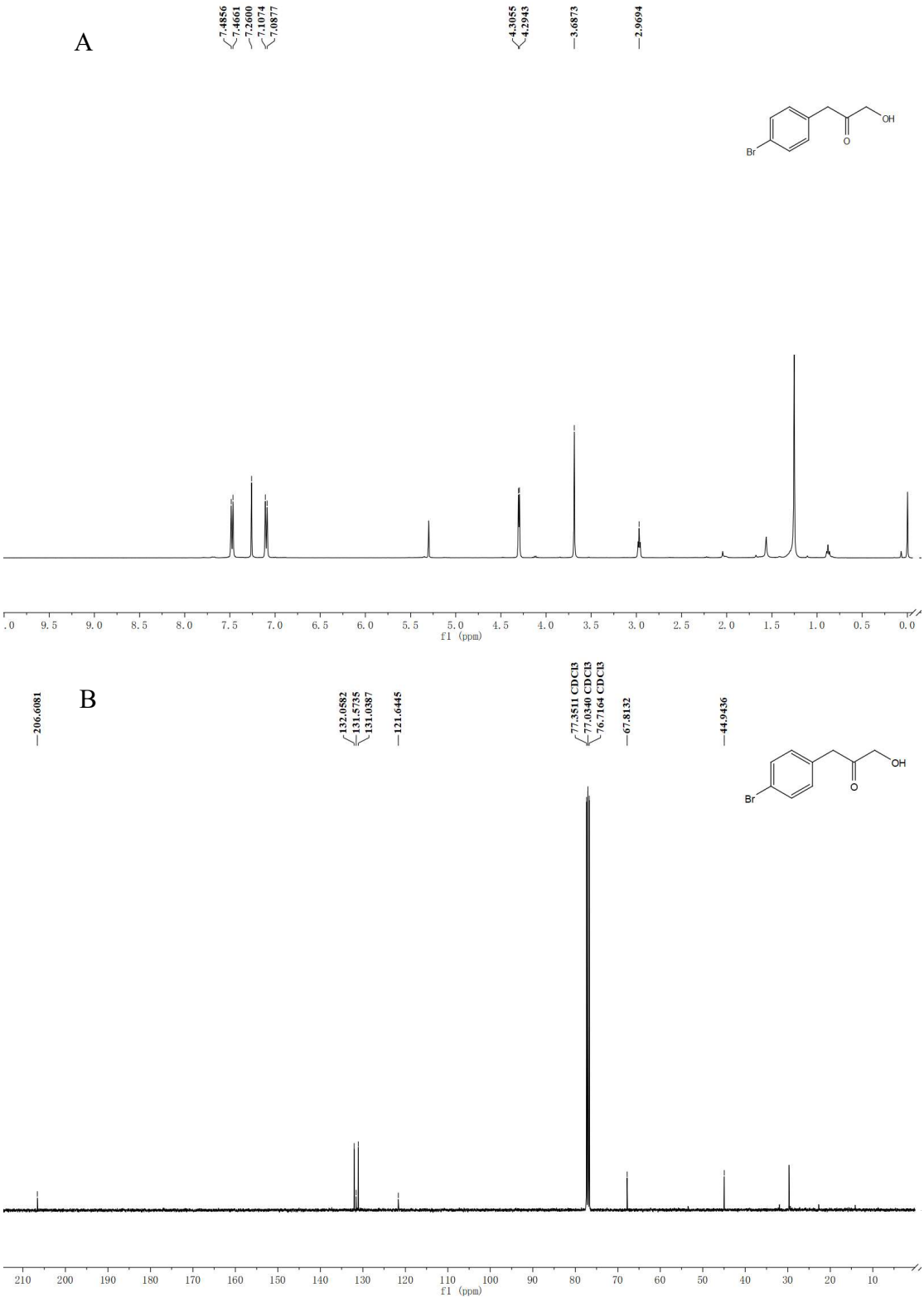

Figure S29. NMR spectra of 1-(4-bromophenyl)-3-hydroxy-2-propanone **4**e. A: ^{1}H-NMR spectra of **4**e; B: ^{13}C-NMR spectra of **4**e.

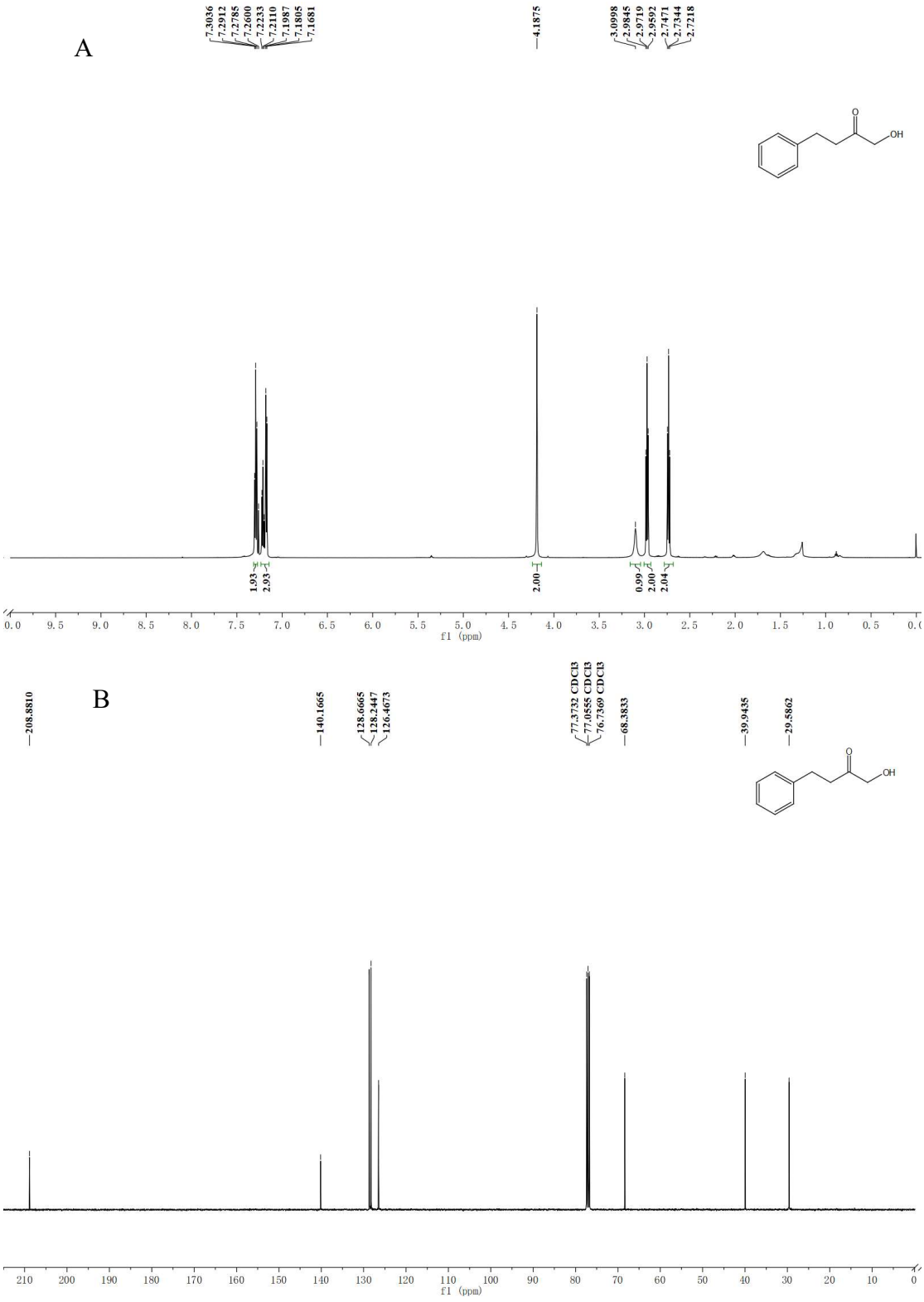

Figure S30. NMR spectra of 1-hydroxy-4-phenyl-2-butanone **4**f. A: ^{1}H-NMR spectra of **4**f; B: ^{13}C-NMR spectra of **4**f.

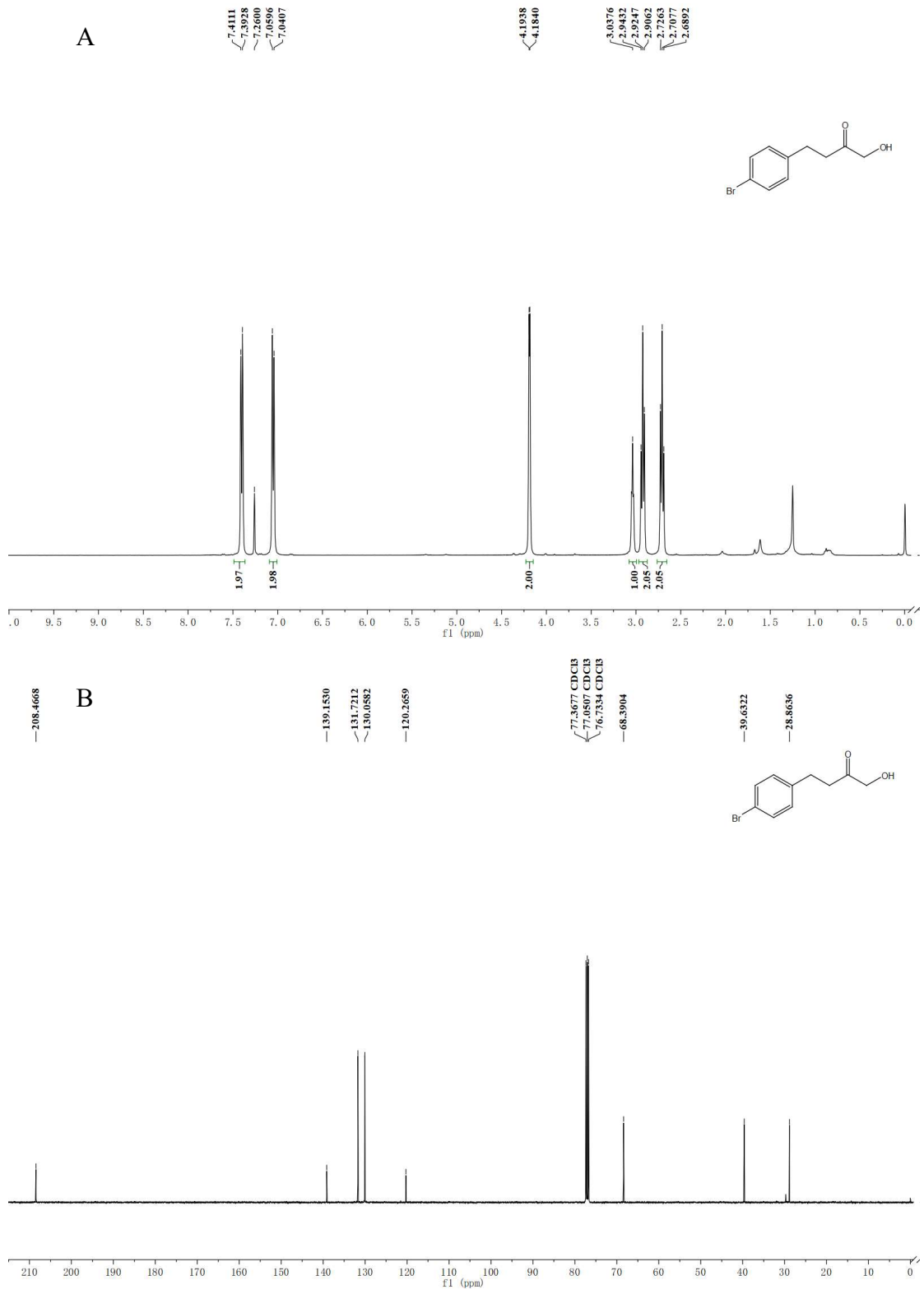

Figure S31. NMR spectra of 4-(4-bromophenyl)-1-hydroxy-2-butanone **4**g. A: ^{1}H-NMR spectra of **4**g; B: ^{13}C-NMR spectra of **4**g.

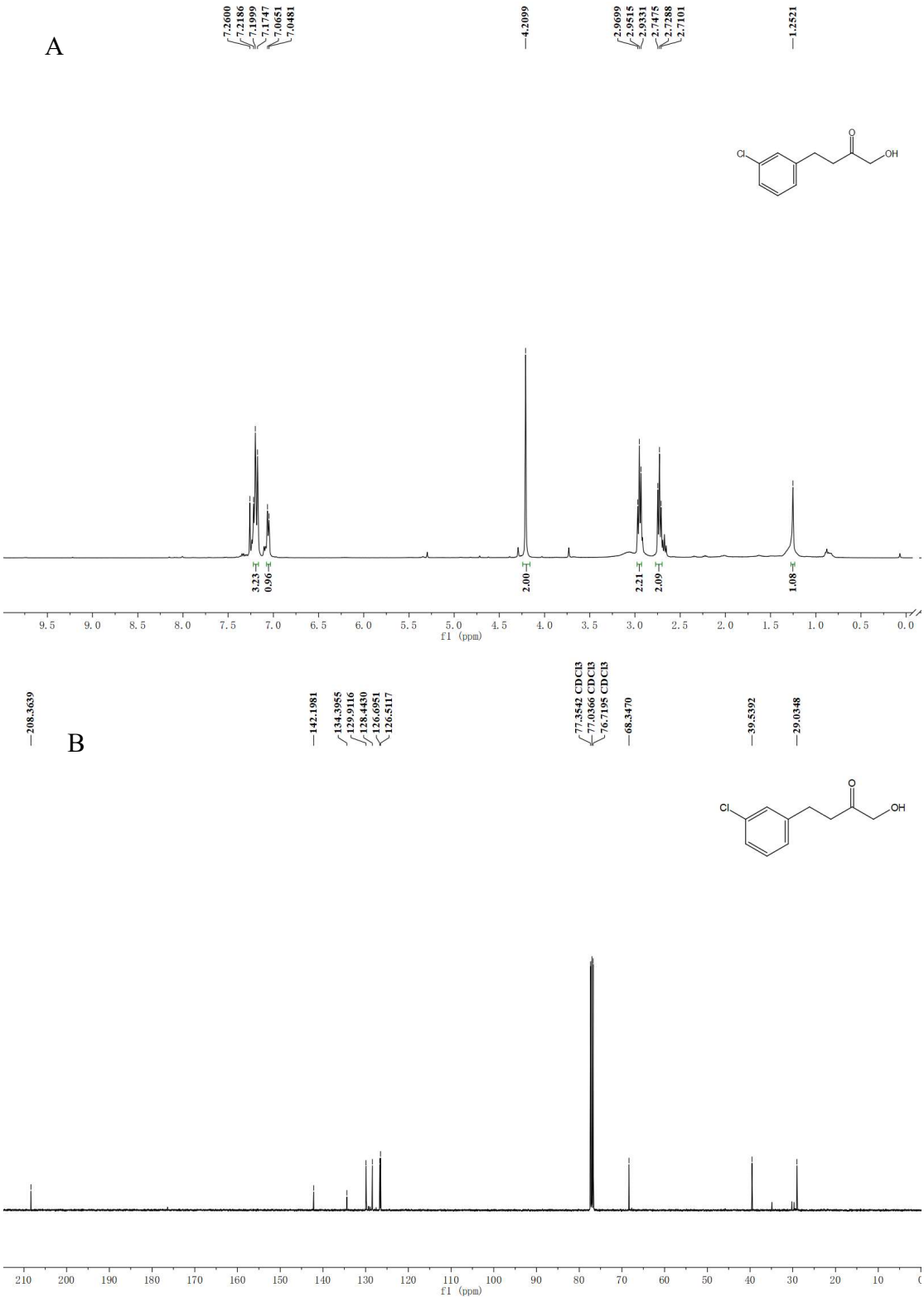

Figure S32. NMR spectra of 4-(3-chlorophenyl)-1-hydroxy-2-butanone **4**h. A: ^{1}H-NMR spectra of **4**h; B: ^{13}C-NMR spectra of **4**h.

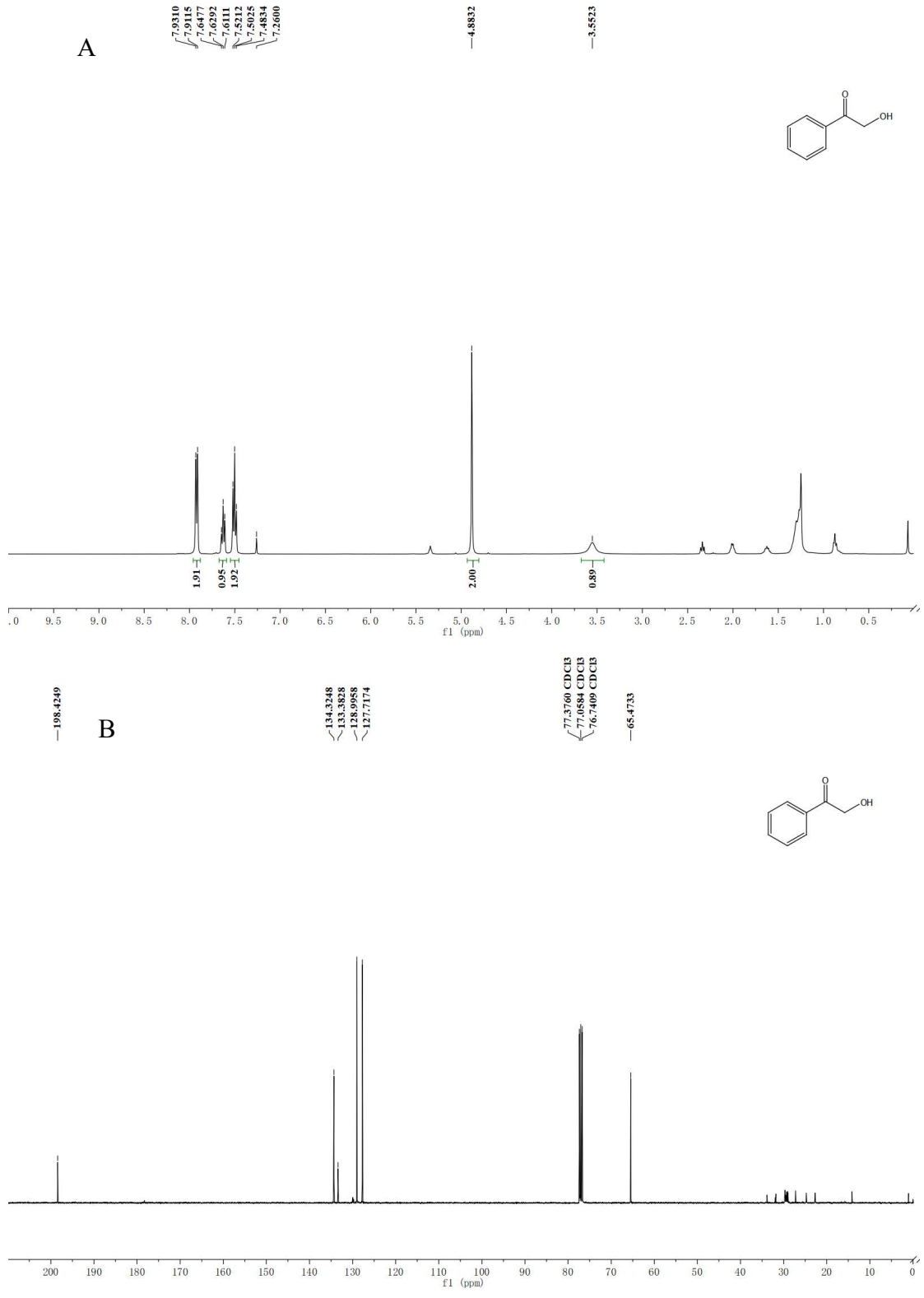

Figure S33. NMR spectra of 2-hydroxyacetophenone **4**i. A: ^{1}H-NMR spectra of **4**i; B: ^{13}C-NMR spectra of **4**i.

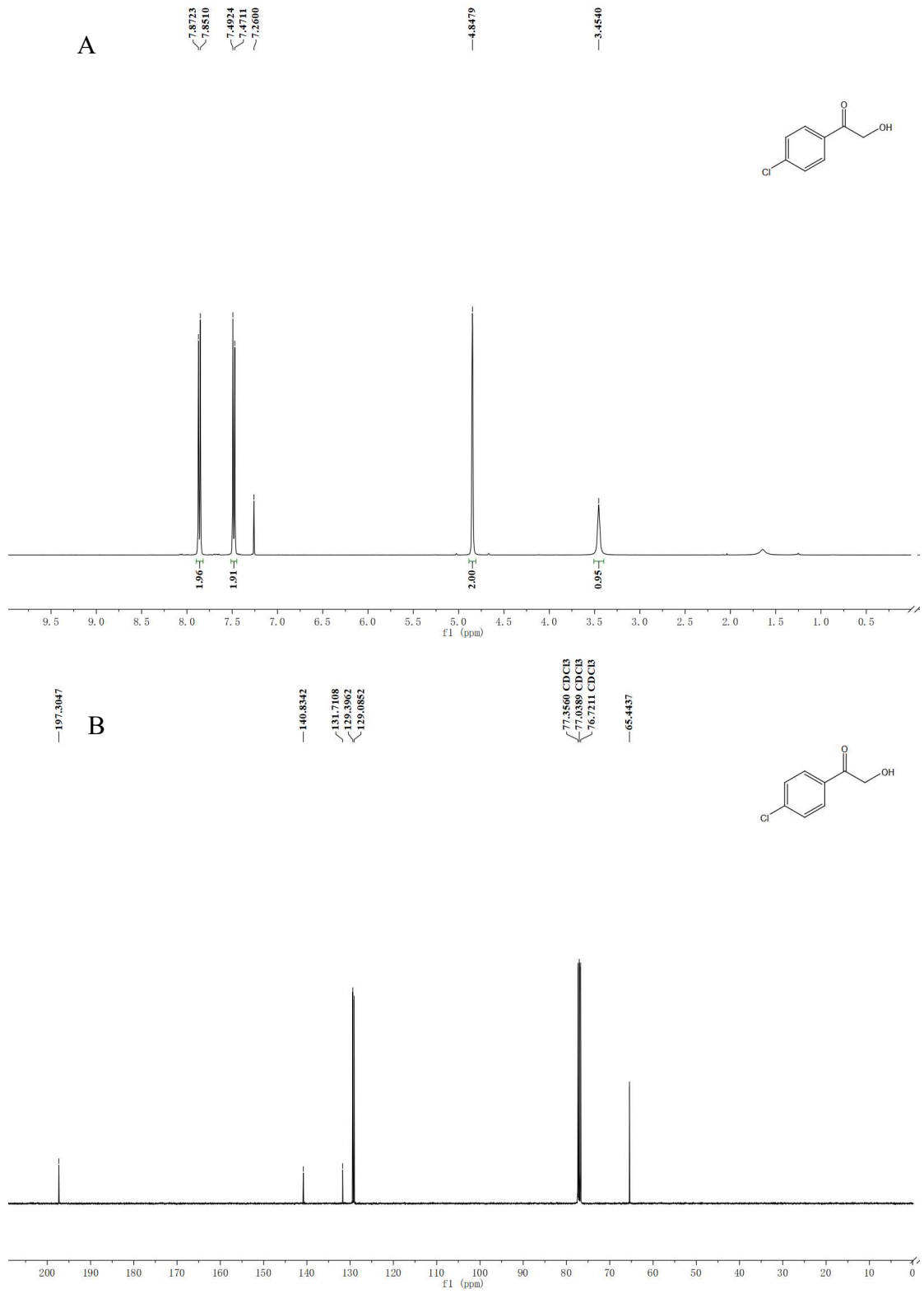

Figure S34. NMR spectra of 1-(4-chlorophenyl)-2-hydroxyethanone **4j**. A: ^{1}H-NMR spectra of **4j**; B: ^{13}C-NMR spectra of **4j**.

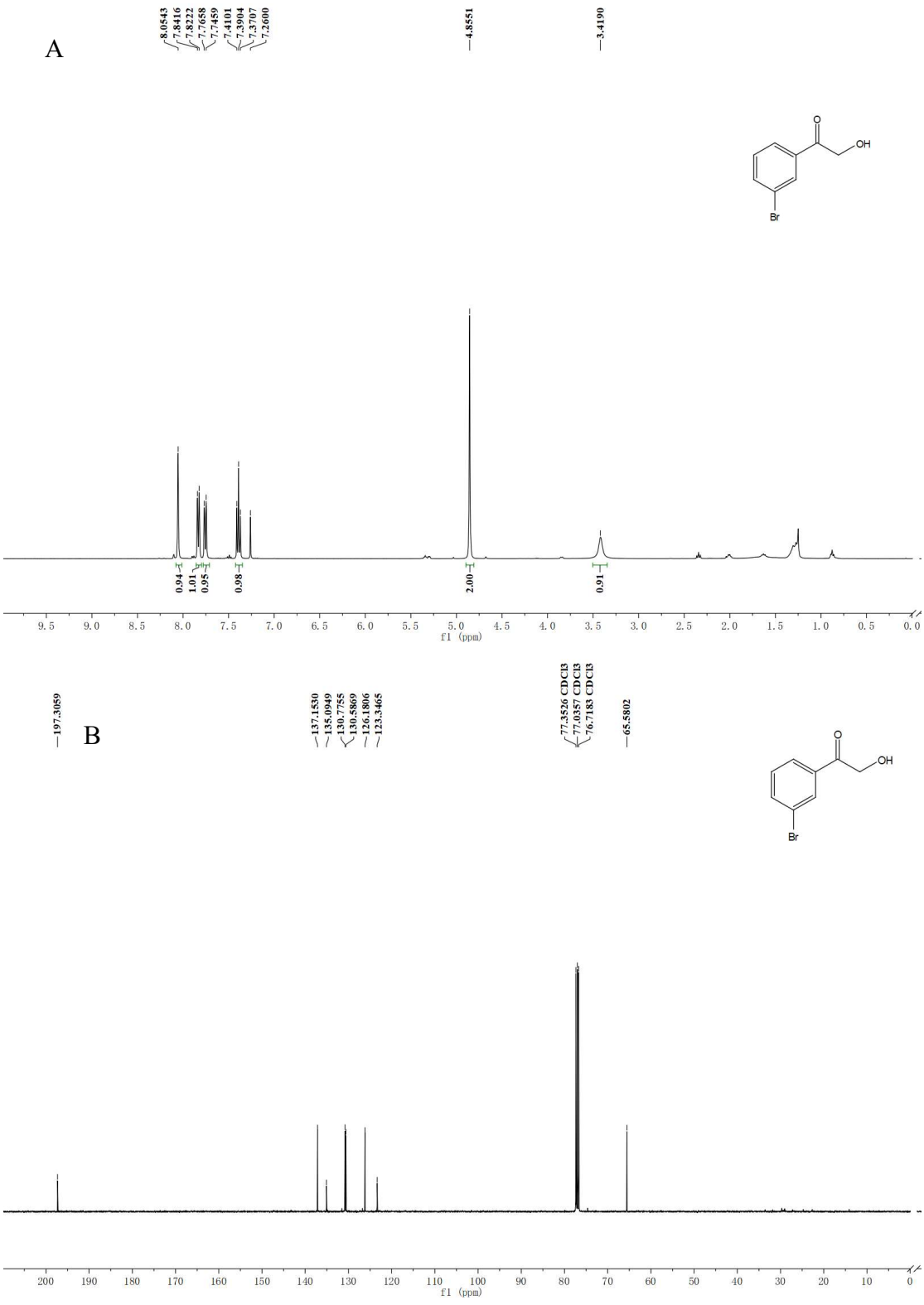

Figure S35. NMR spectra of 1-(3-bromophenyl)-2-hydroxyethanone **4**k. **A:** ^{1}H-NMR spectra of **4**k; **B:**^{13}C-NMR spectra of **4**k.

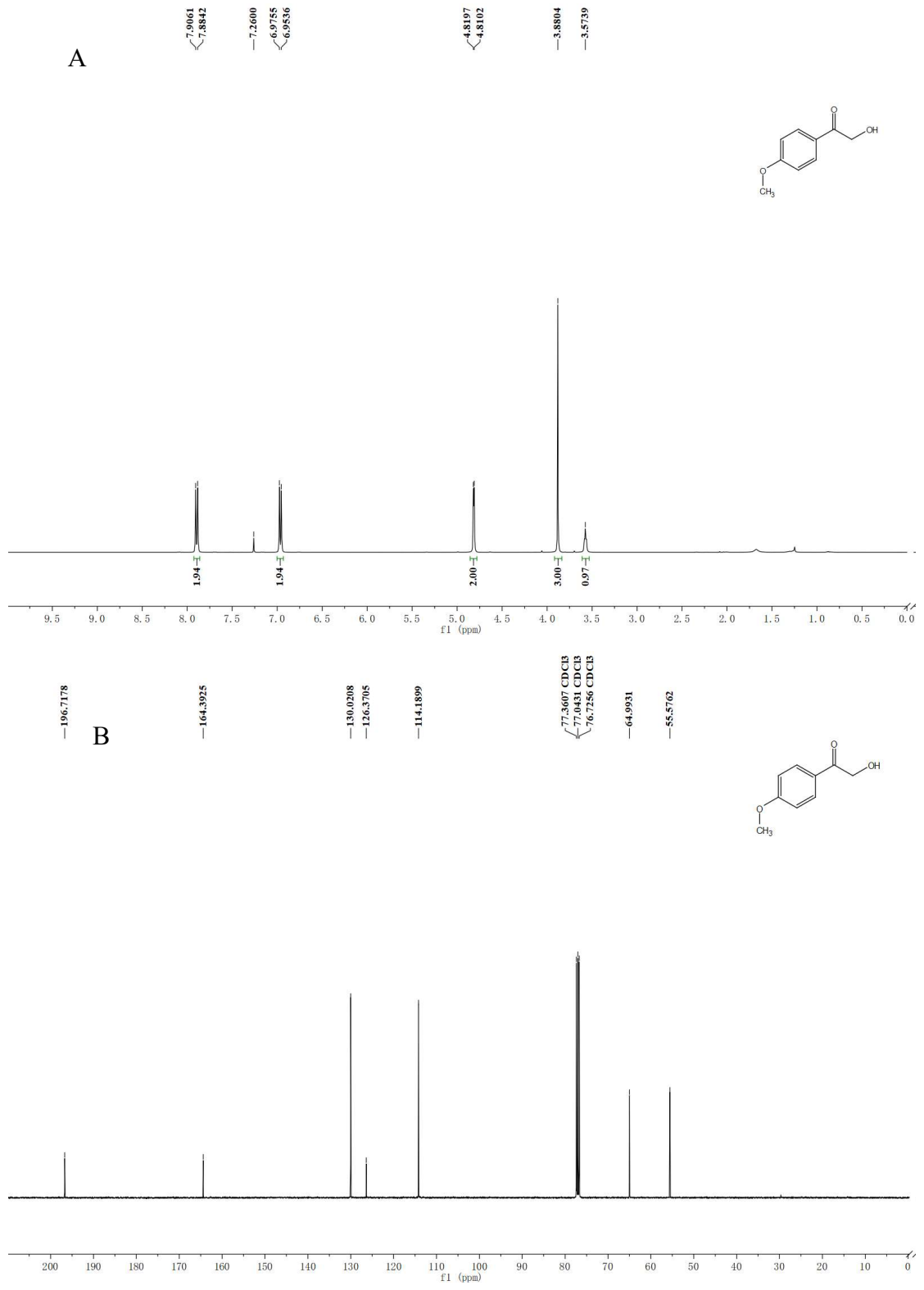

Figure S36. NMR spectra of 2-hydroxy-1-(4-methoxyphenyl)ethanone **4**l. A: ^{1}H-NMR spectra of **4**l; B: ^{13}C-NMR spectra of **4**l.

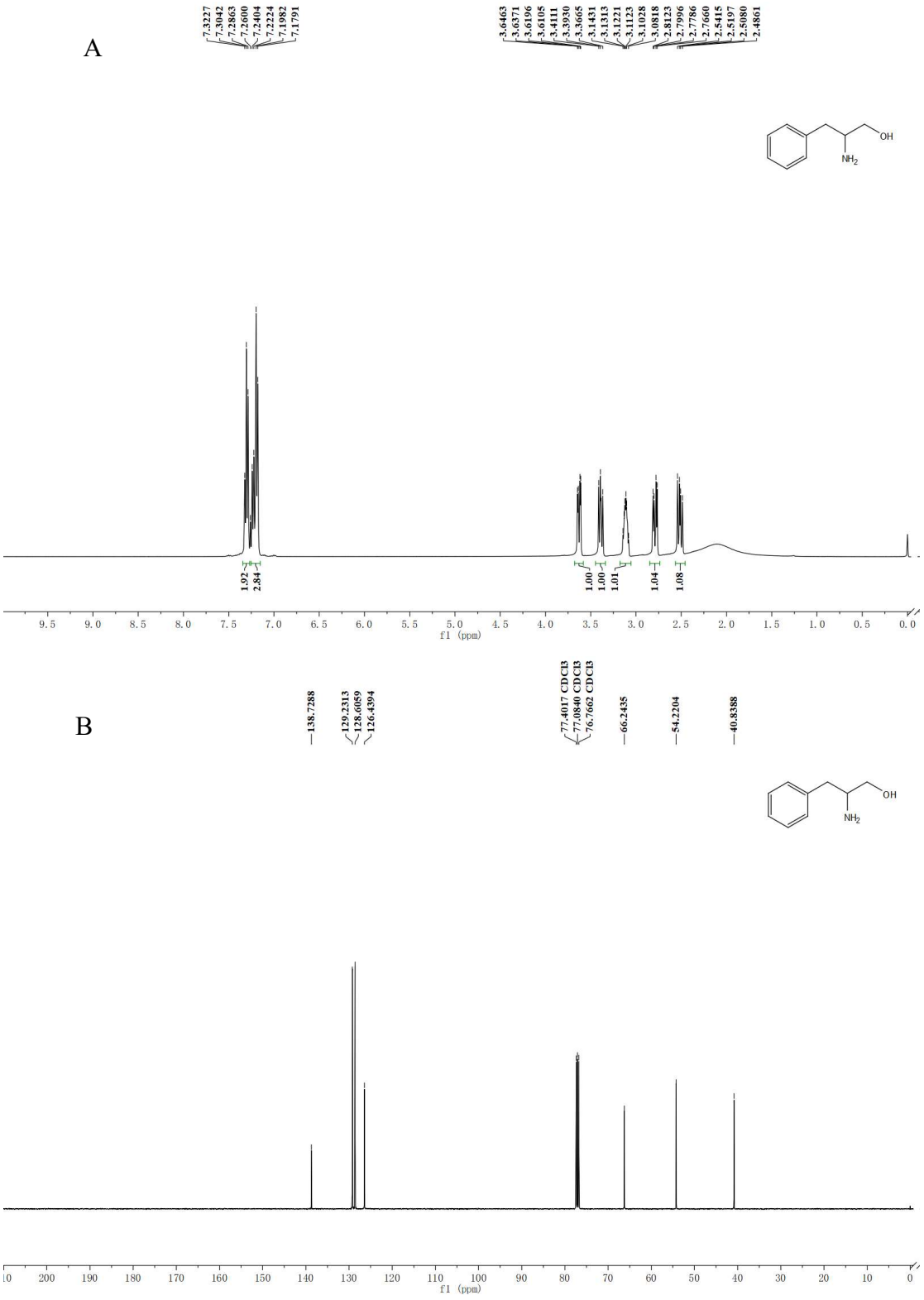

Figure S37. NMR spectra of Phenylalaninol **5**a. A: ^{1}H-NMR spectra of 5a; B: ^{13}C-NMR spectra of 5a.

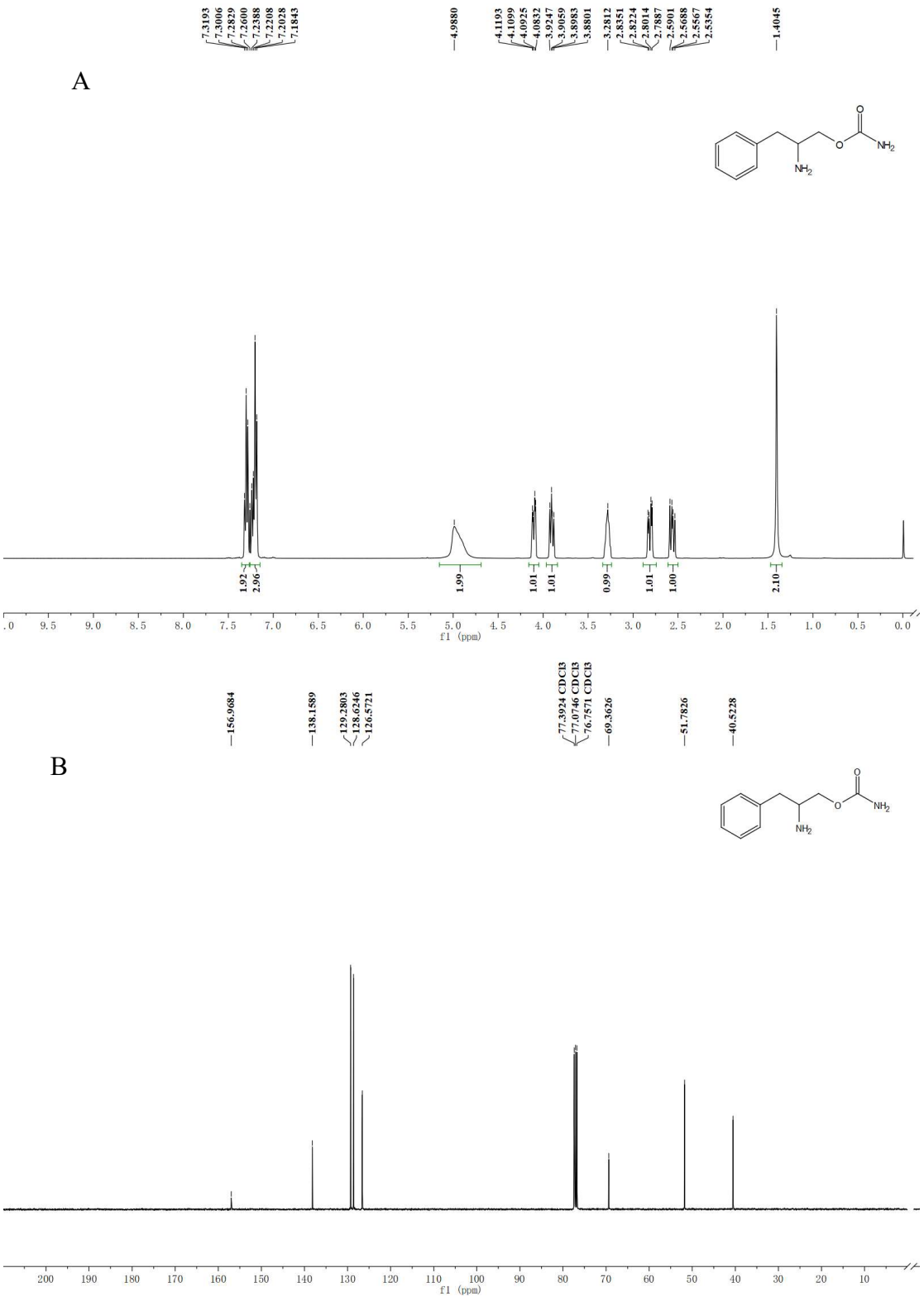

Figure S38. NMR spectra of Solriamfetol. A: ^{1}H-NMR spectra of Solriamfetol; B: ^{13}C-NMR spectra of Solriamfetol.

References

[1] D. P. Pantaleone, A. M. Geller, P. P. Taylor, *J. Mol. Catal. B-Enzym.*, 2001, **11**, 795–803.

[2] Z. Vuralhan, M. A. Morais, S. L. Tai, M. D. W. Piper, J. T. Pronk, *Appl. Environ. Microb.*, 2003, **69**, 4534–4541.

[3] M. M. Bradford, *Anal. Biochem.*, 1976, **72**, 248–254.

[4] J. Abramson, J. Adler, J. Dunger, R. Evans, T. Green, A. Pritzel, O. Ronneberger, L. Willmore, A. J. Ballard, J. Bambrick, S. W. Bodenstein, D. A. Evans, C. C. Hung, M. O'Neill, D. Reiman, K. Tunyasuvunakool, Z. Wu, A. Žemgulytė, E. Arvaniti, C. Beattie, O. Bertolli, A. Bridgland, A. Cherepanov, M. Congreve, A. I. Cowen-Rivers, A. Cowie, M. Figurnov, F. B. Fuchs, H. Gladman, R. Jain, Y. A. Khan, C. M. R. Low, K. Perlin, A. Potapenko, P. Savy, S. Singh, A. Stecula, A. Thillaisundaram, C. Tong, S. Yakneen, E. D. Zhong, M. Zielinski, A. Žídek, V. Bapst, P. Kohli, M. Jaderberg, D. Hassabis, J. M. Jumper, *Nature*, 2024, **630**, 493–500.

[5] E. Chovancova, A. Pavelka, P. Benes, O. Strnad, J. Brezovsky, B. Kozlikova, A. Gora, V. Sustr, M. Klvana, P. Medek, L. Biedermannova, J. Sochor, J. Damborsky, *Plos Comput. Biol.*, 2012, **8**, e1002708.

[6] (a) C. R. Søndergaard, M. H. M. Olsson, M. Rostkowski, J. H. Jensen, *J. Chem. Theory Comput.*, 2011, **7**, 2284–2295; (b) M. H. M. Olsson, C. R. Søndergaard, M. Rostkowski, J. H. Jensen, *J. Chem. Theory Comput.*, 2011, **7**, 525–537.

[7] C. I. Bayly, P. Cieplak, W. D. Cornell, P. A. Kollman, *J. Phys. Chem.*, 1993, **97**, 10269–10280.

[8] (a) J. Eberhardt, D. Santos-Martins, A. F. Tillack, S. Forli, *J. Chem. Inf. Model.*, 2021, **61**, 3891–3898; (b) O. Trott and A. J. Olson, *J. Comput. Chem.*, 2010, **31**, 455–461.

[9] K. J. Bowers, E. Chow, H. Xu, R. Dror, M. Eastwood, B. A. Gregersen, J. L. Klepeis, I. Kolossvary, M. A. Moraes, F. D. Sacerdoti, J. K. Salmon, Y. Shan, D. E. Shaw, In *Proceedings of the 2006 ACM/IEEE conference on Supercomputing*, 2006, 84-es.

[10] S. B. Bhirud, S. Naik, S. K. Mishra, R. B. Kawthekar, D. S. Patekar, N. Patil, PCT patent, WO2020035769A1, 2020.

[11] R. L. Hanson, B. L. Davis, Y. Chen, S. L. Goldberg, W. L. Parker, T. P. Tully, M. A. Montana, R. N. Patel, *Adv. Synth. Catal.*, 2008, **350**, 1367–1375.

[12] U. Kaulmann, K. Smithies, M. E. B. Smith, H. C. Hailes, J. M. Ward, *Enzyme Microb. Tech.*, 2007, **41**, 628–637.

[13] F. G. Mutti, C. S. Fuchs, D. Pressnitz, J. H. Sattler, W. Kroutil, *Adv. Synth. Catal.*, 2011, **353**, 3227–3233.

[14] F. Li, Y. Du, Y. Liang, Y. Wei, Y. Zheng, H. Yu, *ACS Catal.*, 2023, **13**, 422–432.

[15] J. Zhang, H. Gao, L. Gao, M. Cheng, S. Huang, J. Zhang, *Green Chem.*, 2024, **26**, 6160–6171.

[16] J. D. Zhang, J. W. Zhao, L. L. Gao, H. H. Chang, W. L. Wei, J. H. Xu, *J. Biotechnol.*, 2019, **290**, 24–32.

[17] R. C. Anand, Vimal, *Tetrahedron Lett.*, 1998, **39**, 917–918.

[18] K. Van Aken, L. Strekowski, L. Patiny, *Beilstein J. Org. Chem.*, 2006, **2**, 3.